Title: Cyanate distribution and uptake above and within the Eastern Tropical South Pacific Oxygen Deficient Zone

Authors: Brittany Widner*[a,b], Calvin W. Mordy [c,d] and Margaret R. Mulholland[a]

[a] Old Dominion University, Department of Ocean, Earth and Atmospheric Sciences, Norfolk, VA

[b] Woods Hole Oceanographic Institution, Department of Marine Chemistry and Geochemistry, Woods Hole, MA

[c] Joint Institute for the Study of the Atmosphere and Ocean, Box 355672, University of Washington, Seattle, WA 98105-5672, USA

[d] Pacific Marine Environmental Laboratory, NOAA, 7600 Sand Point Way, NE, Seattle WA 98115, USA

*Address all correspondence to
Brittany Widner
Department of Marine Chemistry and Geochemistry
Woods Hole Oceanographic Institution
360 Woods Hole Rd. MS #4
Woods Hole, MA
02543
phone: (216) 554-0102

email: bwidn001@odu.edu

Running head: Cyanate in the ETSP Oxygen Deficient Zone

Keywords: cyanate, nitrogen cycle, oxygen deficient zone, eastern tropical south pacific, urea, anammox, cyanammox

Accepted Article

This is the author manuscript accepted for publication and has undergone full peer review but has not been through the copyediting, typesetting, pagination and proofreading process, which may lead to differences between this version and the Version record. Please cite this article as doi:10.1002/lno.10730.

This article is protected by copyright. All rights reserved.

Abstract

Cyanate is a simple reduced nitrogen (N) compound that can be a source of N and carbon (C) for marine organisms and may also be a substrate for dissimilatory N processes such as nitrification and anammox. We measured cyanate distributions and cyanate and urea uptake in the Eastern Tropical South Pacific (ETSP), a region defined by coastal upwelling, high primary productivity, a shallow oxic layer, and rapid N loss from a large oxygen deficient zone (ODZ). Cyanate concentrations ranged from below the limit of detection (0.4 nM) to 45 nM in the oxic upper water column. Below the oxycline, cyanate concentrations were largely below detection except for small cyanate peaks (2 to 8.3 nM) within the core of the ODZ at some stations. The majority of N taken up in the shallow oxic layer was from ammonium and urea (78 ± 8 %); cyanate uptake was < 2 % of these. Uptake of cyanate fluctuated diurnally with the highest rates of cyanate N uptake in the early afternoon. In the ODZ, rates of cyanate, urea, and ammonium uptake were similar to each other (0.1 to 14 nmol N l^{-1} d^{-1}) and to previously reported rates of $^{15}N_2$ production supported by cyanate and ammonium (3 to 14 nmol N_2 l^{-1} d^{-1}). This suggests a role for cyanate in the metabolism of anaerobic microbes and a potential role for cyanate in the anammox reaction (cyanammox). To our knowledge, these represent the first rates of N uptake in a marine anoxic water column.

Introduction

Simple, reduced, organic N compounds are potentially important sources of N for assimilation and energy in marine systems (Alonso-Sáez et al. 2012; Palatinszky et al. 2015; Sipler and Bronk 2015) and yet little is known about the cycling of many of these compounds in the environment. Cyanate (OCN^-) is perhaps the simplest organic N compound and only recently has a method been developed to measure its concentrations in marine systems (Widner

Accepted Article

This article is protected by copyright. All rights reserved.

et al. 2013). OCN^- is produced during algal decomposition, as a result of photochemical reactions, and through abiotic urea degradation (Dirnhuber and Schutz 1948; Kamennaya et al. 2008; Widner et al. 2016). Urea [$CO(N_2H_2)_2$], another simple organic compound, accounts for approximately one third of nitrogen uptake across all aquatic systems and is released to marine systems by bacteria, fecal pellet leaching, sloppy feeding, zooplankton excretion, atmospheric deposition and anthropogenic sources such as wastewater and fertilizer (Bronk and Steinberg 2008; Mulholland and Lomas 2008; Sipler and Bronk 2015). Because urea and OCN^- are both taken up and produced by marine microbes, their distributions are biologically controlled, similar to those of ammonium (NH_4^+) and nitrite (NO_2^-) (Gruber 2008; Widner et al. 2016; Widner and Mulholland 2017). In the oligotrophic North Atlantic Ocean, we found that urea uptake accounted for up to 50 % of the total measured N uptake while OCN^- uptake accounted for up to 10 % of total N uptake (Widner et al. 2016).

The genetic capacities for urea uptake and intracellular decomposition are widespread among marine microbes, and the gene for intracellular OCN^- decomposition, *cynS*, has been identified in some plants, phytoplankton, bacteria, and archaea (Guilloton et al. 2002). A bacterial OCN^- transporter, *cynABD*, has also been identified in some strains of the ubiquitous marine cyanobacteria *Prochlorococcus* and *Synechococcus* (Palenik et al. 2003; Rocap et al. 2003), and *cynA* expression by these cyanobacterial groups has been observed in marine systems (Kamennaya and Post 2013). Cultured populations of *Synechococcus* WH8102 (Palenik et al. 2003), *Prochlorococcus* MED4 and SB (Kamennaya et al. 2008; Berube et al. 2015), and a dinoflagellate, *Prorocentrum donghaiense* (Hu et al. 2012), have been grown with OCN^- as the sole source of N. In addition, OCN^- and urea have been shown to support nitrification (Alonso-

Accepted Article

This article is protected by copyright. All rights reserved.

Sáez et al. 2012; Palatinszky et al. 2015) and anaerobic ammonium oxidation (Babbin et al. 2017).

The region of the Eastern Tropical South Pacific (ETSP) adjacent to the Peruvian and Northern Chilean coastline is unique in that intense coastal upwelling leads to high rates of primary productivity and consequently the largest tonnage fishery in the world (Pennington et al. 2006). Below these highly productive waters, decomposition of sinking particulate organic matter coupled with poor ventilation of subsurface waters leads to the formation of a permanent oxygen deficient zone (ODZ) where oxygen concentrations are below the limit of detection (10 nM) (Revsbech et al. 2009) and anaerobic microbial metabolisms proliferate. Although the three major oceanic ODZs, in the Eastern Tropical North and South Pacific and Arabian Sea, account for just 0.1 % of the ocean's volume (Codispoti et al., 2001), they are biogeochemically significant because they account for a third of oceanic N losses (Codispoti 2007). In addition, the volume of ODZ waters are projected to expand in the future based on global change scenarios (Stramma et al. 2008) possibly increasing the quantitative significance of reactions happening there. N losses occur via two dissimilatory anaerobic pathways - "canonical" denitrification, a heterotrophic process whereby oxidized nitrogen compounds are reduced to N_2, and anaerobic ammonium oxidation (anammox), a chemoautotrophic process by which NO_2^- and NH_4^+ are converted to N_2 (Dalsgaard et al. 2003; Devol 2008). While N loss and other dissimilatory N processes have been fairly well studied in marine ODZs, to our knowledge, N uptake has not been measured below the euphotic zone and in ODZs. All organisms, including those in ODZs, require N for growth, and competition for N compounds between dissimilatory and assimilatory processes could influence community composition and N speciation, with consequences for controls on N loss.

Accepted Article

This article is protected by copyright. All rights reserved.

Here, we report OCN^- concentrations and uptake rates in the ETSP within and above the ODZ. We compared OCN- concentrations with rates of OCN^- uptake and uptake of urea, NH_4^+, NO_2^-, and nitrate (NO_3^-) in the shallow oxic layer. We also compared the distributions of these compounds with respect to their uptake rates in the ODZ and to previously published rates of $^{15}N_2$ production (Babbin et al. 2017) from OCN^-, urea, and NH_4^+ at this site.

Materials and Methods

Study Site, Sample Collection, and Cyanate and Nutrient Analysis

All measurements and samples were collected during a cruise aboard the *R/V Nathaniel B. Palmer* from June 27 - July 21, 2013. Stations were located in the ETSP between 10 and 22 °S and 70 and 86 °W (Figure 1). Stations occupied during the cruise included two transects, one approximately 200 NM offshore and roughly parallel to the coastline and a second along 17 °S from 79 to 86 °W at 1 ° intervals, and two process stations (BB1 and BB2). Station BB2 was located near the coast within an area experiencing intense coastal upwelling and Station BB1 was further offshore where upwelling intensity was much lower (Figure 1A). Except for station BB2, temperature, salinity, *in situ* chlorophyll *a* (Chl *a*, manufacturer calibration to convert fluorescence to mg m^{-3}), photosynthetically active radiation (PAR, Biospherical), and oxygen (Sea-Bird, SBE 43) were measured using a CTD (Sea-Bird, SBE 911 plus) mounted to a 24-bottle rosette (10 L Niskin bottles). The location of the ODZ (oxygen concentration below detection limit, BDL) was verified using a highly sensitive STOX sensor (detection limit 10 nM), and no oxic intrusions were observed within the ODZ (Revsbech and Garcia-Robledo unpubl.) as has been shown previously in this area (Revsbech et al. 2009; Tiano et al. 2014).

At station BB2, OCN^-, urea, NO_3^-, NO_2^-, and NH_4^+ profiles were collected using an *in situ* pump profiler. The pump profiler was equipped with a CTD package (Sea-Bird, SBE 25)

Accepted Article

This article is protected by copyright. All rights reserved.

and was lowered to 400 m at a rate of 4 m min^{-1}. Water was pumped from depth at 2 L min^{-1}, and samples were collected from the pump outflow at discrete time intervals which corresponded to ~ 4 m sampling resolution. Water was collected for OCN^- and urea analysis in sterile, twice rinsed 50 ml polypropylene tubes, filtered using 0.2 µm nylon filters (sterile, Fisherbrand) attached to 60 ml syringes. For cyanate analysis, the filtrate was transferred to triplicate 2 ml sterile polypropylene microcentrifuge tubes (Thomas Scientific, catalog number 1219F50), and, for urea analysis, the filtrate was transferred to duplicate sterile 15 ml polypropylene tubes. OCN^- samples were stored at -80 °C until derivatization and analysis by high performance liquid chromatography (HPLC) according to Widner et al. (2013) with modifications described in Widner and Mulholland (2017). Urea samples were stored at -20 °C until colorimetric analysis using an Astoria Pacific nutrient autoanalyzer (Price and Harrison 1987) in accordance with the manufacturer's specifications. At all other stations, samples for OCN^- and urea concentrations were collected from the Niskin bottles by gravity filtration through a 0.2 µm membrane filter (Millipore) directly into the 15 ml and 2 ml polypropylene tubes and stored and analyzed as described above. NO_3^-, NO_2^-, and NH_4^+ samples from both the pump profiler and Niskin bottles were collected in 30 ml acid-washed high density polyethylene (HDPE) bottles and analyzed shipboard within 24 hours using a custom nutrient autoanalyzer built from Perstorp, Alpkem and AAII components. At Station BB2, NH_4^+ samples were collected from the pump profiler directly into 60 mL pre-conditioned HDPE bottles and were analyzed using the more sensitive ortho-phthalaldehyde (OPA) method (Holmes et al. 1999). Limits of detection for NO_3^-, NO_2^-, NH_4^+, and urea were 70, 20, 40, and 80 nM, respectively, using the nutrient autoanalyzers, and the limit of detection for NH_4^+ using the OPA method was 10 nM. The limit of detection for cyanate was 0.4 nM (Widner et al. 2013).

Accepted Article

This article is protected by copyright. All rights reserved.

Oxic Uptake Methods

N uptake (NO_3^-, NO_2^-, NH_4^+, urea, and OCN^-) was measured at the surface and Chl *a* maximum at Stations 9 and BB1; NH_4^+, urea, and OCN^- uptake were measured at station BB2. Oxygenated water samples collected from Niskin bottles mounted to the CTD rosette were transferred directly to acid-cleaned 1 L polyethylene terephthalate glycol (PETG) incubation bottles. Uptake experiments were initiated by adding highly enriched (98 %) ^{15}N-labeled NH_4^+, NO_3^-, NO_2^-, and ^{15}N- and ^{13}C-labeled urea and OCN^-. Substrate additions for oxic incubations were targeted to be between 2 and 10 % of the ambient concentrations of NH_4^+, NO_3^-, NO_2^-, urea, and OCN^- to yield reliable and realistic uptake rate measurements (Mulholland et al. 2009). When ambient concentrations were unknown prior to the initiation of experiments (urea and OCN^-) or were < 300 nM (sometimes true for NO_2^- and NH_4^+), 30 nM substrate additions were made, which sometimes led to enrichments ≥ 10 % and may have stimulated uptake: a common problem when environmental nutrient concentrations are in the low nanomolar range (Glibert and Capone 1993; Lipschultz 2008).

Depending on the depth and light level of sample collection, incubation bottles were placed in one of three deck incubators equipped with flow-through seawater and 1, 2, or 4 neutral density screens (55, 28, and 14 % of ambient incident light). To minimize the likelihood of substantial changes in the isotopic composition of the source pool and reaching isotopic equilibrium over the course of incubations, while also allowing adequate time to detect enrichment in the particulate phase, the incubation lengths were as short as possible (2 hours). Incubations were terminated by gentle vacuum filtration onto glass fiber filters (0.7 μm GF/F, ≤ 5 mm Hg) which were rinsed with filtered site water immediately following filtration while the filters were still damp to remove any unincorporated ^{15}N labeled substrate. Filters were then

Accepted Article

This article is protected by copyright. All rights reserved.

stored at -20 °C until analysis. In the laboratory, filters were dried at 40 °C, pelletized in tin capsules and analyzed on a Europa 20/20 isotope ratio mass spectrometer equipped with an automated N and C analyzer. The natural abundances of ^{15}N and ^{13}C in particulate material were measured independently (n=3) at each station and depth. Uptake rates were calculated using a mixing model (Montoya et al. 1996; Mulholland et al. 2006; Mulholland and Lee 2009). Limits of detection for uptake rates were calculated as in Widner and Mulholland (2017).

Kinetics of NH_4^+, urea, and OCN^- uptake were measured at stations BB1 and BB2. $^{15}N^{13}C$ substrate additions ranged from 10 to 1000 nM, and incubations were 2 hours as described above. To determine diurnal variability in OCN^- uptake in surface waters at Station BB2, OCN^- uptake was measured in triplicate uptake experiments initiated approximately every 4 hours over the course of 27 hours. Water for these experiments was collected from the ship's flow-through system as the ship followed a patch of water using floating sediment traps as drogues.

Anoxic Uptake Rates

Uptake rates were determined in anoxic, sub-euphotic waters at Station BB2. Anoxic samples were incubated in duplicate acid-washed, helium-purged, evacuated, 3.8 L, 2-mil thick, polyvinyl fluoride (PVF) transparent gas sampling bags with dual entry points: one a nickel-plated brass hose barb and the other a septum (Tedlar, Cole Parmer EW-01409-92). Water was transferred from Niskin bottles into the bags using tygon tubing attached to the barb. Any helium remaining in the bag after filling was removed by syringe through the septum port. Care was taken to minimize the potential for oxygen contamination. Niskin bottles remained sealed until immediately prior to sampling, and only one 3.8 L bag was filled per 10 L Niskin bottle. Although these bags were used successfully on a previous cruise (Jayakumar et al. 2017), the

Accepted Article

This article is protected by copyright. All rights reserved.

bags used during this cruise were unexpectedly fragile and even with careful handling, approximately 30 % of the bags ruptured leading to loss of replicates. We checked the bags for leaks by visually monitoring fluid loss and checking the transparent bags for the appearance of bubbles during the incubations. Any bags thought to be leaking could have been contaminated for oxygen and were discarded.

For all anoxic incubations, ambient concentrations of urea, NH_4^+, and OCN^- were below the limit of detection (BDL), and substrate additions ranged from 105 to 145 nM N. Consequently, rate estimates may be considered maximum rates. All bags were incubated in the dark at 11 °C in a temperature controlled room. Because some of the anoxic incubations included water from the secondary Chl *a* maximum, uptake by phytoplankton may have been underestimated by incubating them in the dark, however, phytoplankton have been shown to take up reduced N compounds in the dark (Mulholland and Lomas 2008) and PAR was < 0.1% of surface light at the depth of the secondary Chl *a* maximum. Incubation times (12 to 48 hours) were longer than typical uptake incubations (Lipschultz 2008; McCarthy and Bronk 2008) because particle flux, and by extension microbial biomass and growth rates, decreases exponentially with depth below the euphotic zone (Martin et al. 1987). Because N uptake had not previously been measured in anoxic water, each bag was sampled at multiple time points to determine the linearity of uptake over time and the optimal incubation length for future studies. Sub-samples were collected using a peristaltic pump fitted with a GF/F filter (0.7 μm) housed in a 25 mm Swinnex filter holder, and the filtrate was collected to determine the volume filtered at each time point. Filters were placed in cryovials and stored frozen at -20 °C until analysis, as for the oxic samples. Uptake rates were calculated in two ways so that we could compare the rates to previously reported uptake rates and to anammox rate measurements which were made in

Accepted Article

This article is protected by copyright. All rights reserved.

parallel (Babbin et al. 2017). First, a rate was calculated for each time point using the mixing model (hereafter referred to as the standard calculation) described above for the oxic incubations and second, a rate was calculated by fitting a simple linear regression to time courses of N uptake within replicate bags (hereafter referred to as the time series calculation), the typical method for calculating rates of dissimilatory nitrogen processes such as anammox (Dalsgaard et al. 2003).

Ocean Color and Sea Surface Temperature

Ocean color and sea surface temperature data used in this study were produced with the Giovanni online data system, developed and maintained by the National Aeronautic and Space Administration Goddard Earth Sciences Data and Information Services Center (NASA GES DISC) (Acker and Leptoukh 2007).

Results

Results presented in this study include: i) the distribution of nitrogen compounds in the oxic upper water and in the ODZ, and how these distributions vary vertically and horizontally along the transects, with respect to each other, Chl *a* content, oxygen concentration, and density, and between process stations (Figures 2-5); ii) uptake rates of OCN^- in the oxic euphotic zone and comparison of these to uptake of other N compounds (Figures 4-6), OCN^- uptake kinetics (Figure 7), and OCN^- uptake rates over a diurnal cycle (Figure 8); and iii) uptake rates if OCN^-, urea, and NH_4^+ within the ODZ in comparison with rates of the production of N_2 gas (N loss) (Figures 4, 5&9). Mean values are reported as the mean ± standard deviation (SD), for the sample sizes described in the Methods, and sample sizes are indicated with n.

Hydrographic Parameters and Dissolved N Distributions

Surface waters in the study region were generally characterized by cold, high Chl *a* water nearshore and warmer, lower Chl *a* water offshore (Figure 1A, Chl *a* data not shown). Surface

This article is protected by copyright. All rights reserved.

OCN^- concentrations were higher (up to 45 nM) at the northern- and western-most stations of the study region (Figure 1B) where surface water temperatures were also higher (> 20 °C). Above the oxycline, OCN^- concentrations ranged from below the detection limit (0.4 nM) to 45 nM with a mean concentration of 5.2 ± 8.5 nM (n = 286, where each datum is the average of three replicates).

Along the longitudinal transect at 17 ^oS, OCN^- concentrations above the pycnocline were highest near the western-most end of the transect (up to 45 nM) and decreased to less than 10 nM at the eastern end of the transect. In contrast, NO_3^- concentrations above the pycnocline were higher in the eastern portion of the transect (Figure 2). Conversely, on the transect parallel to the coastline, the highest OCN^- and NO_3^- concentrations above the pycnocline co-occurred at the northern end of the transect (Figure 3). Primary NO_2^- maxima (PNM) and NH_4^+ maxima were observed below the Chl *a* maximum throughout the longitudinal transect (Figure 2), but there was no such peak for OCN^- nor was the OCN^- distribution either positively or negatively correlated with the Chl *a* distribution on either transect. Chl *a*, NO_2^-, NH_4^+, and NO_3^- concentrations were generally patchier along the transect parallel to the coastline (Figure 3), as was OCN^-. Elevated NO_2^-, NO_3^-, and OCN^- concentrations were present throughout the mixed layer at the northern end of the transect and NH_4^+ and NO_2^- concentrations were elevated at approximately 19 ^oS relative to adjacent waters, but NO_3^- and OCN^- were not.

Along the longitudinal transect at 17^oS, the ODZ thickened towards the coast, increasing from ~30 m in thickness at the farthest west station (~330- 360 m) to ~250 m thick at the easternmost station (~120 - 370 m; Figure 2). Along the transect parallel to the coastline, the ODZ was 100 to 300 m thick (Figure 3). Secondary nitrite maxima (SNM) were observed at most stations within the ODZ along both transects, and NH_4^+ concentrations were usually BDL

Accepted Article

This article is protected by copyright. All rights reserved.

(DL = 40 nM) below the oxycline (Figures 2&3). OCN^- concentrations in the ODZ were significantly lower than those observed above it ($p<0.001$; 1.4 ± 1.8; $n = 69$) in the ODZ; Figures 2&3). Most of the detectable OCN^- concentrations in the ODZ were concentrated in small peaks in the middle of the ODZ mainly in the western half of the longitudinal transect (< 4 nM) and on both the northern (6.8 nM) and southern (6.4 nM) ends of the transect parallel to the coastline. OCN^- concentrations were <2 nM below 700 m at all stations (Supplemental Information).

At station BB1, Chl *a* was approximately 1 mg m^{-3} in the upper 60 m with a slight maximum centered at 30 m (Figure 4A). The base of the euphotic zone (1% of surface PAR) was at 66 m (data not shown), the nitracline was at 60 m, and the ODZ extended from 120 to 370 m (Figure 4A). NO_3^- concentrations increased with depth below the pycnocline but then decreased between approximately 150 and 350 m, corresponding to an increase in NO_2^- concentrations (Figure 4B). OCN^- and NH_4^+ concentrations were highest in surface waters whereas the highest urea concentrations were in a subsurface maximum at 31 m. While urea and NH_4^+ concentrations peaked at approximately 0.6 and 0.7 μM, respectively, the highest OCN^- concentrations were only 10 nM (Figures 4 C-E). In the upper oxycline, OCN^- and NH_4^+ concentrations decreased to near the limits of detection, although there was a small OCN^- peak within the ODZ (198 m, 3.6 nM).

At station BB2, the base of the euphotic zone (1 % of surface PAR) was at 40 m (data not shown) and the ODZ extended from 90 to 400 m (Figure 5A). There were two Chl *a* maxima, one in the oxic layer at 25 m and one in the ODZ centered at 99 m (Figure 5A) where PAR was < 0.1 % of surface irradiance (Supplemental Information). As for BB1 and the transect stations, NO_3^- increased with depth below the pycnocline but then decreased in concentration within the ODZ corresponding to increased NO_2^- concentrations (Figure 5B). Vertical profiles of

Accepted Article

This article is protected by copyright. All rights reserved.

concentrations and uptake rates for OCN^-, urea, and NH_4^+ are shown in Figures 5 C - E. Although OCN^- concentrations were an order of magnitude lower than those of urea and NH_4^+, the vertical profiles of all three were similar in shape with high surface concentrations, a subsurface minimum, and a maximum at 28 m. The OCN^-, urea, and NH_4^+ maxima were shallower than the PNM (40 m) but slightly deeper than the top of the nitracline (25 m). Concentrations decreased to below detection near the base of the oxic layer, although the decrease in NH_4^+ and urea concentrations with depth was sharper than the decrease in OCN^- concentration.

Cyanate Uptake

At Stations 9 and BB1, OCN^- N uptake in surface waters and at the Chl *a* maximum was less than 2 % of total measured N uptake (NH_4^+, urea, NO_3^-, NO_2^-, and OCN^-) (Figures 4 B-E and 6, Table 1). Yet the OCN^- turnover time was comparable to those of NH_4^+ and urea, except in surface water collected at BB1 where the turnover time of OCN^- was an order of magnitude higher (Table 1). The majority of N taken up in the upper oxic water column was from NH_4^+ and urea with turnover times < 2 days for NH_4^+ and ≤ 8 days for urea (Table 1). At Station BB2, OCN^- uptake in surface water and at the Chl *a* maximum (25 m) was less than 1 % of NH_4^+ and urea uptake (Figure 5). OCN^- and urea C uptake were below the limits of detection at Stations 9 and BB1.

Despite the low ambient OCN^- concentrations, OCN^- uptake was not saturated at 1000 (BB1) or 600 (BB2) nM (Figure 7). While attempted, uptake kinetics could not be determined for urea or NH_4^+ at either station because environmental concentrations of urea and NH_4^+ were already saturating for uptake (Supplemental Information). OCN^- C uptake was BDL in all kinetics experiments but was measureable in diurnal studies. There was significant diurnal

Accepted Article

This article is protected by copyright. All rights reserved.

variability in OCN^- uptake at Station BB2 for both N and C uptake (Figure 8). Both volumetric and Chl *a* -normalized N uptake from OCN^- were highest in the afternoon (7/19 13:30), and uptake was significantly higher (Student's t-test, n=2, $p < 0.05$) at similar times on the second day (0.25 ± 0.12 nmol N l^{-1} h^{-1} at 16:20) than on the first day (0.04 ± 0.01 nmol N l^{-1} h^{-1} at 15:45) suggesting substantial daily variability in its uptake. OCN^- C uptake showed a different pattern. Volumetric and Chl *a* -normalized C uptake was higher at night than during the day. However, we also observed daily variability in OCN^- C uptake; higher uptake rates were observed on the first day (0.3 ± 0.02 nmol C l^{-1} h^{-1}) than on the second day (BDL; < 0.02 nmol C l^{-1} h^{-1}) at nearly the same time (mid-afternoon).

For ODZ N uptake rates calculated using the standard calculation (Montoya et al. 1996; Mulholland et al. 2006; Mulholland and Lee 2009), there were no significant differences in uptake rates between the first and second time points for all substrates (NH_4^+, OCN^-, and urea) and depths (95, 230, and 400 m) with one exception; NH_4^+ uptake at 95 m was lower at the shorter time point (8 hours) compared to the longer time point (36 hours, Figure 9, Table 2), possibly indicating stimulation of uptake by the substrate addition. Uptake rates were linear for pooled replicate bags over the three time points as determined using the time series calculation (linear regression of N taken up over time for significance criterion $\alpha = 0.05$), except for OCN^- at 95 m and NH_4^+ at 400 m (Figure 9, Table 2). ^{15}N enrichment in the particulate phase after the first time point (time point A) was sufficient to detect N uptake rates using the standard calculation (Table 2), and shorter incubations are less susceptible to erroneous rate calculations resulting from changing biomass, community composition, and isotopic composition of the source pool during the incubation ("bottle effects"; Lipschultz 2008).

Accepted Article

This article is protected by copyright. All rights reserved.

At Station BB2, N (OCN^-, urea and NH_4^+) and C (OCN^- and urea) uptake were measured at three depths in the ODZ: just below the oxycline (95 m), at the SNM depth (230 m), and at the base of the ODZ (400 m) (Figures 5 C-E and 11, Table 2). Urea C uptake was BDL at all ODZ depths, and OCN^- C uptake was BDL at all depths and time points except in samples collected from 95 m after 36 hours when the rate was 1.4 ± 0.8 pmol C l^{-1} h^{-1}, a low but detectable rate. N uptake was detected at all depths in the ODZ, despite the fact that concentrations of all three compounds were below the limits of detection throughout the ODZ (Figures 5 C-E). For the uptake rate calculated from time point A using the standard calculation, NH_4^+ uptake was highest at the depth of the SNM, but urea and OCN^- N uptake rates increased with depth within the ODZ and were highest at the base of the ODZ. OCN^- N uptake was of similar magnitude throughout the water column while urea and NH_4^+ uptake were 1 to 2 orders of magnitude higher in surface waters than in the ODZ (Figures 5D and 5E). In the ODZ, N uptake rates of OCN^-, urea, and NH_4^+ were similar in magnitude to each other.

Discussion

Oxic Processes

The shallow, euphotic oxic region sampled in the ETSP was characterized by NO_3^- concentrations in the low micromolar range, elevated OCN^- concentrations relative to deeper waters, patchy NO_2^- and NH_4^+ concentrations, and high concentrations of Chl *a*. Micromolar surface DIN concentrations are typical for this region due to the balance between inputs from nutrient-rich upwelled equatorial waters, thermocline shoaling, coastal upwelling, and drawdown from high productivity (Montecino and Lange 2009, Pennington et al. 2006). OCN^- concentrations were mostly uniform with depth above the pycnocline, but were BDL below the pycnocline with the exception of small maxima within the ODZ at some stations. OCN^- uptake

Accepted Article

This article is protected by copyright. All rights reserved.

was a small fraction of N uptake in euphotic, oxic water (< 2 %), and OCN^- uptake was not saturated at 1 μM OCN^- concentrations. In contrast, urea and NH_4^+ uptake were saturated at low concentrations. From this we infer that OCN^- did not contribute significantly to the N demand of phytoplankton in this system at this time of year.

OCN^- concentrations in late summer (August) in the coastal North Atlantic between Cape Hatteras and the Gulf of Maine ranged from 0 to 25 nM (Widner et al. 2016; Widner and Mulholland 2017); however, in the ETSP, OCN^- concentrations were at or near the limit of analytical detection at most stations and depths measured. The North American Atlantic coastal region is an N-limited, temperate system influenced by western boundary currents with a relatively wide continental shelf and a mixed, seasonally dynamic phytoplankton community (Townsend et al. 2006; Pan et al. 2011). In contrast, the ETSP lies in a tropical Eastern boundary current and has a narrow continental shelf, experiences regular coastal upwelling, diatom dominance, and offshore iron limitation (Franz et al. 2012, Hutchins et al. 2002, Montecino and Lange 2009, Pennington et al. 2006). At stations on the continental shelf slope in the coastal North Atlantic, the OCN^- concentration was less than 2 nM in surface waters and there was an OCN^- maximum below the Chl *a* maximum followed by a gradual decline in OCN^- concentration with depth (Widner et al. 2016; Widner and Mulholland 2017). In contrast, we observed relatively high OCN^- concentrations in ETSP surface waters (10 to 45 nM) that rapidly declined below the pycnocline, and there were no subsurface maxima associated with the Chl *a* maximum. OCN^- profiles in the coastal North Atlantic were attributed to uptake in sunlit surface waters, production by degrading organic matter at intermediate depths as it sank out of the euphotic zone, and possible oxidation of OCN^- with depth. The concentration of a dissolved compound in seawater reflects the balance of its production and consumption, and in the ETSP,

Accepted Article

This article is protected by copyright. All rights reserved.

the more uniform, higher OCN^- concentrations in the euphotic zone likely reflect higher rates of OCN^- production in the ETSP than in the North Atlantic. OCN^- uptake rates in the upper oxic layer of the ETSP (0.1 ± 0.1 nmol N l^{-1} h^{-1}) were an order of magnitude lower than uptake rates in the North Atlantic in August (1.1 ± 1.0 nmol N l^{-1} h^{-1}; Widner and Mulholland 2017), and diatoms, which are dominant in the ETSP (Franz et al. 2012; Pennington et al. 2006) but not in the North Atlantic in August (Pan et al. 2011), have been shown to produce cyanate in culture (Widner et al. 2016). The regional difference in OCN^- profile shape may also reflect very different stratification and mixing regimes between the two locations. In the North Atlantic in August (summer), stations were highly stratified (average mixed layer depth (MLD) 8 ± 5 m) and the Chl *a* maximum and the base of the euphotic zone (1% PAR) were much deeper than the MLD. Conversely, in the ETSP in July (austral winter) the water column was less stratified (average MLD 72 ± 22 m) and the depths of the Chl *a* maximum and base of the euphotic zone were more similar to and often shallower than the MLD. Along that same transect, water density and NO_3^- concentrations above the pycnocline were higher in the east than in the west (Figure 2), suggesting coastal upwelling, which is common in this region (Montecino and Lange 2009). Increases in surface OCN^- concentrations along the western half of the longitudinal 17 ^oS transect could have resulted from the degradation of Chl *a* biomass as productive upwelled water advected offshore.

OCN^- N uptake rates at the surface and Chl *a* maximum in the coastal ETSP were an order of magnitude lower (0.1 ± 0.1 nmol l^{-1} h^{-1}, n = 29, 1 cruise) than those observed in the coastal North Atlantic Ocean (1.3 ± 1.9 nmol l^{-1} h^{-1}, n = 135, 4 cruises; Widner and Mulholland 2017). In both studies, OCN^- uptake was usually a small fraction of total N uptake; however, in the oligotrophic North Atlantic, OCN^- N was up to 10 % of total N uptake (Widner et al. 2016)

Accepted Article

This article is protected by copyright. All rights reserved.

suggesting that OCN^- may be a quantitatively more important source of N in oligotrophic systems than in nutrient-rich coastal upwelling systems (Kamennaya and Post 2013). Stations 9 and BB1 were on the edge of the Peruvian coastal upwelling region, typically dominated by diatoms (Franz et al. 2012) that are thought to prefer NO_3^- as a N source (Mulholland and Lomas 2008). In studies of N uptake, NO_3^- N is often refered to as "new" N because it is largely introduced to the euphotic zone from deep water, while reduced N compounds such as NH_4^+ and DON, including urea and cyanate, are regenerated within the euphotic zone. The ratio of "new" N uptake to total N ("new" + "regenerated") uptake is termed the f-ratio (Eppley and Peterson 1979), and previous studies have reported that "new" N uptake (NO_3^- uptake) was roughly 50% of total N uptake in coastal upwelling systems, which equates to an f-ratio of ~ 0.5 (Wilkerson and Dugdale 2008). In the present study, NO_3^- accounted for 10- 29 % of total measured N uptake (NO_3^- + NO_2- + NH_4^+ + urea + cyanate), while regenerated N (NO_2^- + NH_4^+ + urea + cyanate) accounted for 70 - 89 % of total measured N uptake. Not all previous studies included forms of recycled N other than NH_4^+, which likely inflated reported f-ratios. However, a similar f-ratio to that reported here (0.1 to 0.29) was observed in euphotic waters at the center of the Peruvian coastal upwelling region (0.1 to 0.36), where the f-ratio was calculated from NH_4^+ and NO_3^- uptake rates and corrected for *in situ* production of those compounds (Fernández et al. 2009). Additionally, many studies, including ours, did not include dinitrogen fixation in calculating the f-ratio, which would be another "new" N source and increase the f-ratio if quantitatively significant. NO_3^- uptake rates from this study (1.7 - 4.2 nmol N l^{-1} h^{-1}) were two orders of magnitude lower than those previously reported for upwelling regions (Wilkerson and Dugdale 2008 and references therein), possibly because our stations were located on the edge of the upwelling region, as can be seen by elevated sea surface temperatures (Figure 1).

Accepted Article

This article is protected by copyright. All rights reserved.

OCN^- N uptake in surface waters was highest at midday, while OCN^- C uptake in surface waters was highest at night, independent of diel changes in Chl *a* concentration (Figure 8). Phytoplankton N demand is likely highest during the day when photosynthetic C uptake is greatest, and uptake of organic reduced C compounds at night could augment photosynthetic C uptake by mixotrophic microbes or supply C to obligate heterotrophs. However, unlike most organic C, OCN^- C cannot be assimilated by heterotrophs, because OCN^- C is in the oxidized form and is converted to CO_2 without a change in oxidation state by the cyanase enzymes (Taussig 1960). Uptake of OCN^- solely as a C source would be an inefficient and unlikely process because dissolved CO_2 concentrations in seawater are three orders of magnitude higher than the highest concentrations of cyanate observed to date in marine systems. Despite this impracticality, autotrophs could assimilate OCN^- C opportunistically if they take up OCN^- for utilization of OCN^- N. OCN^- N is converted to NH_4^+ by the intracellular cyanase enzyme (Taussig 1960) and is presumably then available for either assimilation or dissimilatory processes.

The night-time increase in uptake of OCN^- C relative to uptake of OCN^- N in surface waters (Figure 8) could be explained by nocturnal uptake of OCN^- C by chemoautotrophic nitrifiers as they utilize OCN^- N as a source of reductant. A cultured terrestrial ammonia oxidizer has the gene for cyanase and was shown to oxidize OCN^- N to NO_2^- in culture (Palatinszky et al. 2015). All sequenced NO_2^- oxidizers have the genes for OCN^- utilization which could indicate OCN^- assimilation or "reciprocal feeding" whereby NO_2^- oxidizers supply ammonia oxidizers, which lack a cyanate utilization pathway, with NH_4^+ via OCN^- decomposition (Spang et al. 2012; Palatinszky et al. 2015). Marine ammonia oxidation in the euphotic zone has been shown to be higher at night than during the day which could be because

Accepted Article

This article is protected by copyright. All rights reserved.

there is reduced competition with phytoplankton at night (Smith et al. 2014) or because of photoinhibition of ammonia oxidation during the day (Hooper and Terry 1974). Night-time ammonia oxidation in surface waters could explain the presence of archaeal ammonia oxidation genes and transcripts there (Church et al. 2010; Santoro et al. 2010; Pedneault et al. 2014). Our results suggest that, in ETSP surface waters, OCN^- N is taken up during the day, probably by photoautotrophs, and that uptake of OCN^- C at night may reflect assimilation of this C by chemoautotrophs which use the OCN^- N for a dissimilatory process, likely ammonia oxidation.

Anoxic Processes

OCN^-, urea, and NH_4^+ uptake were also measured below the euphotic zone in the ODZ, and uptake rates of these compounds increased with depth and exceeded rates of anammox attributed to those same substrates at the SNM (Fig. 5; Babbin et al. 2017). Uptake rates of all three N compounds were of similar magnitude within the ODZ (0.1 - 0.5 nmol N l^{-1} h^{-1}; Fig. 5, Table 2). In contrast, the uptake rates of OCN^- in the euphotic zone were one to two orders of magnitude lower than those of NH_4^+ and urea (Table 1). The nonlinear N uptake for OCN^- at 95 m and NH_4^+ at 400 m (Table 2) over the incubation time course could have resulted from high variability between incubation bags, possibly caused by variable oxygen contamination or low sample size. For future studies of ODZ N uptake, where only one time point is logistically feasible, we recommend incubation lengths of 8 to 12 hours to maximize detection of enrichment in the particulate phase but to minimize "bottle" effects. Much longer incubations are likely needed to detect C uptake, if there is any, although our 24-48 hour incubations failed to detect C uptake in all incubations but one (detection limit < 1 pmol N $l^{-1}h^{-1}$).

Uptake rates at the base of the oxycline coincided with a small secondary Chl *a* peak that has been attributed to low light adapted *Prochlorococcus* that are typically found near the base of

This article is protected by copyright. All rights reserved.

the oxycline and are known to be able to utilize OCN^- (Goericke et al. 2000; Lavin et al. 2010; Kamennaya and Post 2013). Nitrogen uptake is typically measured in sunlit waters where nitrogen limits phytoplankton growth and reproduction and consequently rates of primary production (Mulholland and Lomas 2008). To our knowledge, nitrogen uptake has not been measured in the mesopelagic zone. However, important heterotrophic and chemoautotrophic biogeochemical processes take place in ODZs (Paulmier and Ruiz-Pino 2009) and the N and C uptake observed in this study may represent N assimilation supporting the growth of these organisms, some of which are autotrophs. Our 105 to 145 nM N additions could have stimulated NH_4^+, urea, and OCN^- uptake in the ODZ, but these rates do demonstrate the potential for uptake by the anoxic microbial community. Denitrifiers are more responsive to episodic nutrient additions than are anammox bacteria (Ward et al. 2009), however N assimilation supporting the growth of these microbial communities has not been widely examined. NO_3^- and NO_2^- are more abundant than reduced N compounds in ODZs, but assimilation of oxidized N compounds is energetically expensive compared to reduced forms of N (Berges and Mulholland 2008; Mulholland and Lomas 2008).

While it is often assumed that N taken up in incubation experiments is assimilated, it could also reflect accumulation of intracellular NH_4^+ in the anammoxosome to support anammox (van Niftrik et al. 2004). NH_4^+ concentrations were below the limit of analytical detection (40 nM at most stations and 10 nM at Station BB2) within the ODZ, as has been observed previously in marine ODZs. These low concentrations were attributed to oxidation of NH_4^+ to N_2 by anammox (Dalsgaard et al. 2012; Galán et al. 2009). NH_4^+ produced by intracellular degradation of OCN^- and urea to NH_4^+ (Miller and Espie 1994; Solomon et al. 2010) could also be shunted to the anammox reaction if anammox bacteria are capable of taking up and degrading OCN^- and

Accepted Article

This article is protected by copyright. All rights reserved.

urea. Urea can degrade abiotically in aqueous solutions to OCN^- (Dirnhuber and Schutz 1948), and OCN^- degrades abiotically to NH_4^+ (Amell 1956; Kamennaya et al. 2008). So it is possible that NH_4^+ produced from OCN^- and urea extracellularly, either biotically or abiotically, was rapidly taken up by the anammox bacteria. While these indirect pathways of OCN^- and urea utilization by anammox organisms are plausible, abiotic reactions are slow and a two-step process is not likely to be linear over short time scales. The linear production of $^{29}N_2$ over 12 hours following the addition of $OC^{15}N^-$ suggests that OCN^- is used directly by anammox bacteria in a "cyanammox" pathway (Babbin et al. 2017). In contrast to OCN^-, there was a 36 hour lag in $^{29}N_2$ production from ^{15}N-urea (Babbin et al. 2017), suggesting that this pathway involves a slow conversion of urea to OCN^- or NH_4^+ followed by OCN^--supported or traditional anammox.

OCN^- C is in the oxidized form and is therefore only available for autotrophic assimilation, and because uptake of OCN^- solely for C assimilation is an inefficient process, OCN^- C is likely only taken up by autotrophs that can utilize OCN^- N. This limitation can explain the low OCN^- C uptake rates observed in this study (≤ 0.001 nmol l^{-1} h^{-1}) as compared to higher rates of OCN^- N uptake and "cyanammox" (~ 0.1 nmol N l^{-1} h^{-1}; Table 2; Babbin et al. 2017). Because anammox is an intracellular process (van Niftrik et al. 2004), the chemoautotrophic bacteria capable of "cyanammox" could potentially assimilate CO_2 derived from OCN^- C throughout the ODZ. However OCN^- C uptake was only detected at 95 m, where it could have been taken up by *Prochlorococcus* which is generally found in the secondary Chl *a* maximum in ODZs (Figure 7A) (Lavin et al. 2010). Some *Prochlorococcus* strains can utilize OCN^- (Rocap et al. 2003; Kamennaya and Post 2013), although whether theses strains are present in the ETSP ODZ is not known.

Accepted Article

This article is protected by copyright. All rights reserved.

OCN^-, urea, and NH_4^+ were taken up and supported anammox in the ODZ despite the fact that these compounds were below their limits of detection, suggesting that the community was "primed" for utilization of these compounds and that there is a tight coupling between production and consumption of these compounds. NH_4^+ is produced in ODZs by degradation of organic matter (Devol 2008), and both OCN^- and urea have been shown to be produced by similar pathways in oxic environments (Sipler and Bronk 2015; Widner et al. 2016). Organic matter degradation could explain the OCN^- maxima observed at some stations within the ODZ, however particle flux and nutrient remineralization decrease exponentially with depth (Martin et al. 1987), and the anoxic OCN^- maxima were deep (~300 m) suggesting consumption of OCN^- in excess of production in the upper ODZ. In previous studies done in oxic waters, the vertical distribution of OCN^- was similar in shape to those of NO_2^- and NH_4^+ suggesting release by phytoplankton or production from degrading organic matter (Widner et al. 2016; Widner and Mulholland 2017; A. Post pers. comm.). NH_4^+ and urea are also supplied to marine systems by zooplankton excretion (Sipler and Bronk 2015), and OCN^- forms from abiotic urea decomposition (Dirnhuber and Schutz 1948). Diurnal vertical migration of zooplankton into ODZs may increase N loss through the anammox pathway by 13% from excretion of NH_4^+ alone (Bianchi et al. 2014). Inputs of OCN^- and urea from zooplankton excretion to the ODZ could further enhance rates of N loss through the cyanammox process. However, rates of zooplankton excretion may be reduced under anoxic conditions (Kiko et al. 2015), so the magnitude of this flux is unknown.

Summary

Here we demonstrate that urea and ammonium are taken up at higher rates than cyanate in the euphotic zone, but all three compounds were taken up at comparable rate in the ODZ in

Accepted Article

This article is protected by copyright. All rights reserved.

the Eastern Tropical South Pacific. We made, to our knowledge, the first measurements of cyanate, urea, and ammonium uptake in an oxygen deficient zone, and these were of similar magnitude to previously reported anammox and "cyanammox" rates.

Acknowledgements

We would like to acknowledge B.B. Ward and A.H. Devol for inviting us to participate on the cruise, B.X. Chang for assistance with ammonium sample collection and analysis, and E. Garcia-Robledo and N.P. Revsbech for measuring nanomolar O_2 concentrations in the incubation bags and in the water column. We also thank O. Ulloa and G. Alarcón for access to and assistance with the pump profiling system. We also thank the captain and crew of the *R/V Nathaniel B. Palmer* for assistance in sampling. This work was funded by NSF grants to MRM and NSF grant 1233425 to CWM. It was partially funded by the Joint Institute for the Study of the Atmosphere and Ocean (JISAO) under NOAA Cooperative Agreements NA17RJ1232 and NA10OAR4320148, and is contribution 2016-01-45 to JISAO and contribution 4567 to NOAA's Pacific Marine Environmental Laboratory.

Accepted Article

This article is protected by copyright. All rights reserved.

Accepted Article

References

Acker, J. G. and G. Leptoukh 2007. Online analysis enhances use of NASA earth science data. Eos, Transactions American Geophysical Union. 88: 14-17

Alonso-Sáez, L., A. S. Waller, D. R. Mende, K. Bakker, H. Farnelid, P. L. Yager, C. Lovejoy, J.-É. Tremblay, and others. 2012. Role for urea in nitrification by polar marine Archaea. Proc. Natl. Acad. Sci. U.S.A. 109: 17989-17994

Amell, A. R. 1956. Kinetics of the hydrolysis of cyanic acid. J. Am. Chem. Soc. 78: 6234-6238

Armbrust, E. V., J. A. Berges, C. Bowler, B. R. Green, D. Martinez, N. H. Putnam, S. Zhou, A. E. Allen, and others. 2004. The genome of the diatom Thalassiosira pseudonana: ecology, evolution, and metabolism. Science. 306: 79-86

Babbin, A. R., B. D. Peters, C. W. Mordy, B. Widner, K. L. Casciotti and B. B. Ward 2017. Multiple metabolisms constrain the anaerobic nitrite budget in the Eastern Tropical South Pacific. Global Biogeochem. Cycles. DOI: 10.1002/2016GB005407.

Berges, J. A. and M. R. Mulholland 2008. Enzymes and Nitrogen Cycling, p. In D. G. Capone, D. A. Bronk, M. R. Mulholland and E. J. Carpenter [eds.], Nitrogen in the Marine Environment. Academic Press.

Berube, P. M., S. J. Biller, A. G. Kent, J. W. Berta-Thompson, S. E. Roggensack, K. H. Roache-Johnson, M. Ackerman, L. R. Moore, and others. 2015. Physiology and evolution of nitrate acquisition in Prochlorococcus. ISME J. 9: 1195-1207

Bianchi, D., A. R. Babbin and E. D. Galbraith 2014. Enhancement of anammox by the excretion of diel vertical migrators. Proc. Natl. Acad. Sci. U.S.A. 111: 15653-15658

Bowler, C., A. E. Allen, J. H. Badger, J. Grimwood, K. Jabbari, A. Kuo, U. Maheswari, C. Martens, and others. 2008. The Phaeodactylum genome reveals the evolutionary history of diatom genomes. Nature. 456: 239-244

Bronk, D. A. and D. K. Steinberg 2008. Nitrogen Regeneration, p. 385-467. In D. G. Capone, D. A. Bronk, M. R. Mulholland and E. J. Carpenter [eds.], Nitrogen in the Marine Environment. Elsevier.

Cho, B. C. and F. Azam 1995. Urea decomposition by bacteria in the Southern California Bight and its implications for the mesopelagic nitrogen cycle. Mar. Ecol.: Prog. Ser. 122: 21-26

Church, M. J., B. Wai, D. M. Karl and E. F. DeLong 2010. Abundances of crenarchaeal amoA genes and transcripts in the Pacific Ocean. Environ. Microbiol. 12: 679-688

Codispoti, L. A. 2007. An oceanic fixed nitrogen sink exceeding 400 Tg N a? 1 vs the concept of homeostasis in the fixed-nitrogen inventory. Biogeosciences. 4: 233-253

Cole, C. A., Z. Wang, T. P. Snow and V. M. Bierbaum 2015. Gas-phase chemistry of the cyanate ion, OCN. The Astrophysical Journal. 812: 77

Dalsgaard, T., D. E. Canfield, J. Petersen, B. Thamdrup and J. Acuna-Gonzalez 2003. N2 production by the anammox reaction in the anoxic water column of Golfo Dulce, Costa Rica. Nature. 422: 606-608

Dalsgaard, T., B. Thamdrup, L. Farías, N. P. Revsbech 2012. Anammox and denitrification in the oxygen minimum zone of the eastern South Pacific. Limnol. Oceanogr. 57:1331-1346

Danger, G., L. Boiteau, H. Cottet and R. Pascal 2006. The peptide formation mediated by cyanate revisited. N-carboxyanhydrides as accessible intermediates in the decomposition of N-carbamoylamino acids. J. Am. Chem. Soc. 128: 7412-7413

This article is protected by copyright. All rights reserved.

Danger, G., S. Charlot, L. Boiteau and R. Pascal 2012. Activation of carboxyl group with cyanate: peptide bond formation from dicarboxylic acids. Amino Acids. 42: 2331-2341

Devol, A. H. 2008. Denitrification Including Anammox, p. 263-301. In D. G. Capone, D. A. Bronk, M. R. Mulholland and E. J. Carpenter [eds.], Nitrogen in the Marine Environment. Elsevier.

Dirnhuber, P. and F. Schutz 1948. The isomeric transformation of urea into ammonium cyanate in aqueous solutions. Biochem. J. 42: 628-632

Eppley, R. W. and B. J. Peterson 1979. Particulate organic matter flux and planktonic new production in the deep ocean. Nature. 282: 677-680

Ferris, J. P., R. A. Sanchez and L. E. Orgel 1968. Studies in prebiotic synthesis III. Synthesis of pyrimidine from cyanoacetylene and cyanate. J. Mol. Biol. 33: 693-704

Franz, J., G. Krahmann, G. Lavik, P. Grasse, T. Dittmar, U. Riebesell 2012. Dynamics and stoichiometry of nutrients and phytoplankton in waters influenced by the oxygen minimum zone in the eastern tropical Pacific. Deep-Sea Res., Part I. 62: 20-31

Fernández, C., L. Farías, and M. E. Alcaman 2009. Primary production and nitrogen regeneration processes in surface waters of the Peruvian upwelling system. Prog. Oceanogr. 83: 159-168

Galán, A., V. Molina, B. Thamdrup, D. Woebken, G. Lavik, M.M.M. Kuypers, and O. Ulloa 2009. Anammox bacteria and anaerobic oxidation of ammonium in the oxygen minimum zone off northern Chile. Deep-Sea Res., Part II. 56: 1021-1031

Glibert, P. M. and D. G. Capone 1993. Mineralization and Assimilation in Aquatic, Sediment, and Wetland Systems, p. 243-268. In R. Knowles and T. H. Blackburn [eds.], Nitrogen Isotope Techniques. Academic Press, Inc.

Goericke, R., R. J. Olson and A. Shalapyonok 2000. A novel niche for *Prochlorococcus* sp. in low-light suboxic environments in the Arabian Sea and the Eastern Tropical North Pacific. Deep-Sea Research I. 47: 1183-1205

Gruber, N. 2008. The marine nitrogen cycle: Overview and Challenges, p. 1-50. In D. G. Capone, D. A. Bronk, M. R. Mulholland and E. J. Carpenter [eds.], Nitrogen in the marine environment. Elsevier.

Guilloton, M., G. S. Espie and P. M. Anderson 2002. What is the role of cyanase in plants?, p. 57-79. In A. Goyal, S. L. Mehta and M. L. Lodha [eds.], Reviews in Plant Biochemistry and Biotechnology. Society for Plant Biochemistry and Biotechnology.

Hagan, W. J., A. Parker, A. Steuerwald and M. Hathaway 2007. Phosphate solubility and the cyanate-mediated synthesis of pyrophosphate. Origins Life Evol. Biosphere. 37: 113-112

Holmes, R. M., A. Aminot, R. Kerouel, B. A. Hooker and B. J. Peterson 1999. A simple and precise method for measuring ammonium in marine and freshwater ecosystems. Canadian Journal of Fisheries and Aquatic Sciences. 56: 1801-1808

Hooper, A. B. and K. R. Terry 1974. Photoinactivation of ammonia oxidation in Nitrosomonas. J. Bacteriol. 119: 899-906

Hutchins, D. A., C. E. Hare, R. S. Weaver, Y. Zhang, G. F. Firme, G. R. DiTullio, M. B. Alm, S. F. Riseman and others 2002. Phytoplankton iron limitation in the Humboldt Current and Peru Upwelling. Limnol. Oceanogr. 47: 997-1011

Hu, Z., M. R. Mulholland, S. Duan and N. Xu 2012. Effects of nitrogen supply and its composition on the growth of *Prorocentrum donghaiense*. Harmful Algae. 13: 72-82

Accepted Article

This article is protected by copyright. All rights reserved.

Jayakumar, A., B.X. Chang, B. Widner, P. Bernhardt, M.R. Mulholland, B.B. Ward 2017. Biological nitrogen fixation in the oxygen-minimum region of the eastern tropical North Pacific ocean. ISME J. DOI: 10.1038/ismej.2017.97.

Jones, M. E. and F. Lipmann 1960. Chemical and enzymatic synthesis of carbamyl phosphate. Proc. Natl. Acad. Sci. U.S.A. 46: 1194-1205

Kamennaya, N. A., M. Chernihovsky and A. F. Post 2008. The cyanate utilization capacity of marine unicellular cyanobacteria. Limnol. Oceanogr. 53: 2485-2494

Kamennaya, N. A. and A. F. Post 2011. Characterization of Cyanate Metabolism in Marine Synechococcus and Prochlorococcus spp. Appl. Environ. Microbiol. 77: 291-301

Kamennaya, N. A. and A. F. Post 2013. Distribution and expression of the cyanate aquisition potential among cyanobacterial populations in oligotrophic marine waters. Limnol. Oceanogr. 58: 1959-1971

Kiko, R., H. Hauss, F. Buchholz and F. Melzner 2015. Ammonium excretion and oxygen respiration of tropical copepods and euphausiids exposed to oxygen minimum zone conditions. Biogeosciences Discuss. 12: 17329-17366

Lavin, P., B. González, J. Santibánez, D. J. Scanlan and O. Ulloa 2010. Novel lineages of *Prochlorococcus* thrive within the oxygen minimum zone of the eastern tropical South Pacific. Environmental microbiology reports. 2: 728-738

Lipschultz, F. 2008. Isotope tracer methods for studies of the marine nitrogen cycle, p. 1345-1384. In D. G. Capone, D. A. Bronk, M. R. Mulholland and E. J. Carpenter [eds.], Nitrogen in the marine environment. Elsevier.

Martin, J. H., G. A. Knauer, D. M. Karl and W. W. Broenkow 1987. VERTEX: carbon cycling in the northeast Pacific. Deep Sea Research Part A. Oceanographic Research Papers. 34: 267-285

McCarthy, M. D. and D. A. Bronk 2008. Analytical Methods for the Study of Nitrogen, p. 1219-1276. In D. G. Capone, D. A. Bronk, M. R. Mulholland and E. J. Carpenter [eds.], Nitrogen in the Marine Environment. Academic Press.

Miller, A. G. and G. S. Espie 1994. Photosynthetic metabolism of cyanate by the cyanobacterium *Synechococcus* UTEX-625. Arch. Microbiol. 162: 151-157

Miller, S. L. and M. Parris 1964. Synthesis of pyrophosphate under primitive earth conditions. Nature. 204: 1248-1250

Montecino, V. and C.B. Lange 2009. The Humboldt Current System: Ecosystem components and processes, fisheries, and sediment studies. Prog. Oceanogr. 83: 65-79

Montoya, J. P., M. Voss, P. Kaehler and D. G. Capone 1996. A simple, high precision tracer assay for dinitrogen fixation. Applied Environmental Microbiololgy. 62: 986-993

Mulholland, M. R., P. W. Bernhardt, C. A. Heil, D. A. Bronk and J. M. O'Neil 2006. Nitrogen fixation and release of fixed nitrogen by *Trichodesmium* spp. in the Gulf of Mexico. Limnol. Oceanogr. 51: 1762-1776

Mulholland, M. R., G. E. Boneillo, P. W. Bernhardt and E. C. Minor 2009. Comparison of Nutrient and Microbial Dynamics over a Seasonal Cycle in a Mid-Atlantic Coastal Lagoon Prone to Aureococcus anophagefferens (Brown Tide) Blooms. Estuaries Coasts. 32: 1176-1194

Mulholland, M. R. and C. Lee 2009. Peptide hydrolysis and the uptake of dipeptides by phytoplankton. Limnol. Oceanogr. 54: 856-868

Accepted Article

This article is protected by copyright. All rights reserved.

Mulholland, M. R. and M. W. Lomas 2008. Nitrogen Uptake and Assimilation, p. 303-384. In D. G. Capone, D. A. Bronk, M. R. Mulholland and E. J. Carpenter [eds.], Nitrogen in the marine environment. Elsevier.

Palatinszky, M., C. Herbold, N. Jehmlich, M. Pogoda, P. Han, M. von Bergen, I. Lagkouvardos, S. M. Karst, and others. 2015. Cyanate as an energy source for nitrifiers. Nature. 524: 105-108

Palenik, B., B. Brahamsha, F. W. Larimer, M. Land, L. Hauser, P. Chain, J. Lamerdin, W. Regala, and others. 2003. The genome of a motile marine *Synechococcus*. Nature. 424: 1037-1042

Pan, X., A. Mannino, H. G. Marshall, K. C. Filippino and M. R. Mulholland 2011. Remote sensing of phytoplankton community composition along the northeast coast of the United States. Remote Sensing of Environment. 115: 3731-3747

Paulmier, A. and D. Ruiz-Pino 2009. Oxygen minimum zones (OMZs) in the modern ocean. Prog. Oceanogr. 80: 113-128

Pedneault, E., P. E. Galand, M. Potvin, J.-É. Tremblay and C. Lovejoy 2014. Archaeal amoA and ureC genes and their transcriptional activity in the Arctic Ocean. Scientific reports. 4:

Pennington, J. T., K. L. Mahoney, V. S. Kuwahara, D. D. Kolber, R. Calienes and F. P. Chavez 2006. Primary production in the eastern tropical Pacific: A review. Prog. Oceanogr. 69: 285-317

Price, N. M. and P. J. Harrison 1987. Comparison of methods for the analysis of dissolved urea in seawater. Mar. Biol. 94: 307-317

Revsbech, N. P., L. H. Larsen, J. Gundersen, T. Dalsgaard, O. Ulloa and B. Thamdrup 2009. Determination of ultra-low oxygen concentrations in oxygen minimum zones by the STOX sensor. Limnology and Oceanography: Methods. 7: 371-381

Rocap, G., F. W. Larimer, J. Lamerdin, S. Malfatti, P. Chain, N. A. Ahlgren, A. Arellano, M. Coleman, and others. 2003. Genome divergence in two *Prochlorococcus* ecotypes reflects oceanic niche differentiation. Nature. 424: 1042-1047

Santoro, A. E., K. L. Casciotti and C. A. Francis 2010. Activity, abundance and diversity of nitrifying archaea and bacteria in the central California Current. Environ. Microbiol. 12: 1989-2006

Sipler, R. E. and D. A. Bronk 2015. Dynamics of Dissolved Organic Nitrogen, p. In D. A. Hansell and C. A. Carlson [eds.], Biogeochemistry of Marine Dissolved Organic Matter. Academic Press.

Smith, J. M., F. P. Chavez and C. A. Francis 2014. Ammonium uptake by phytoplankton regulates nitrification in the sunlit ocean. PloS one. 9: e108173

Solomon, C. M., J. L. Collier, G. M. Berg and P. M. Glibert 2010. Role of urea in microbial metabolism in aquatic ecosystems: a biochemical and molecular review. Aquat. Microb. Ecol. 59: 67-88

Spang, A., A. Poehlein, P. Offre, S. Zumbrägel, S. Haider, N. Rychlik, B. Nowka, C. Schmeisser, and others. 2012. The genome of the ammonia-oxidizing CandidatusNitrososphaera gargensis: insights into metabolic versatility and environmental adaptations. Environ. Microbiol. 14: 3122-3145

Taussig, A. 1960. The synthesis of the induced enzyme, cyanase, in *E. coli*. Biochim. Biophys. Acta. 44: 510-519

Accepted Article

This article is protected by copyright. All rights reserved.

Tiano, L., E. Garcia-Robledo, T. Dalsgaard, A. H. Devol, B. B. Ward, O. Ulloa, D. E. Canfield and N. P. Revsbech 2014. Oxygen distribution and aerobic respiration in the north and south eastern tropical Pacific oxygen minimum zones. Deep Sea Res., Part I. 94: 173-183

Townsend, D. W., A. C. Thomas, L. M. Mayer, M. A. Thomas and J. A. Quinlan 2006. Oceanography of the Northwest Atlantic continental shelf (1, W), p. 119-168. In A. R. Robinson and K. H. Brink [eds.], The Sea. Harvard University Press.

van Niftrik, L., J. Fuerst, J. S. Sinningh Damste, G. Kuenen, M. S. M. Jetten and M. Strous 2004. The anammoxasome: an intracytoplasmic compartment in anammox bacteria. FEMS Microbiol. Lett. 233: 7-13

Ward, B., A. Devol, J. Rich, B. Chang, S. Bulow, H. Naik, A. Pratihary and A. Jayakumar 2009. Denitrification as the dominant nitrogen loss process in the Arabian Sea. Nature. 461: 78-81

Widner, B. and M. R. Mulholland 2017. Cyanate distribution and uptake in North Atlantic coastal waters. Limnol. Oceanogr. doi: 10.1002/lno.10588

Widner, B., M. R. Mulholland and K. Mopper 2013. Chromatographic Determination of Nanomolar Cyanate Concentrations in Sea and Estuarine Waters by Precolumn Fluorescence Derivatization. Anal. Chem. 85: 6661-6666

Widner, B., M. R. Mulholland and K. Mopper 2016. Distribution, Sources, and Sinks of Cyanate in the Coastal North Atlantic Ocean. Environmental Science & Technology Letters.

Wilkerson, F. P. and R. C. Dugdale 2008. Coastal Upwelling, p. 771-807. In D. G. Capone, D. A. Bronk, M. R. Mulholland and E. J. Carpenter [eds.], Nitrogen in the marine environment. Elsevier.

Yamagata, Y. 1999. Prebiotic formation of ADP and ATP from AMP, calcium phosphates and cyanate in aqueous solution. Origins Life Evol. Biosphere. 29: 511-520

Yamagata, Y. and T. Mohri 1982. Formation of cyanate and carbamyl phosphate by electric discharges of model primitive gas. Origins of Life. 12: 41-44

Accepted Article

This article is protected by copyright. All rights reserved.

Accepted Article

751 **Tables**

752 Table 1. Uptake rates, turnover times, and ambient concentrations of nitrate (NO_3^-), nitrite (NO_2^-), ammonium (NH_4^+), urea, and
753 cyanate (OCN^-) for stations BB1 and 9. Values below the limit of detection are indicated as BDL, and turnover times that could not
754 be calculated because the uptake rate or concentration was BDL are listed as N/A. Average deviations (n =2) are shown in
755 parentheses.

Station	Latitude (°S)	Longitude (°E)	Depth (m)		NO_3^-	NO_2^-	NH_4^+	Urea	OCN^-
BB1	13.711	-81.390	2.5	Uptake (nmol N l^{-1} h^{-1})	4.2(0.8)	0.04(0.0)	7.8(0.1)	2.4(0.7)	.01(0.0)
				Concentration (µM N)	2.4	0.2	0.3	0.3	0.01
				Turnover Time (days)	24	170	1.6	4.9	36
BB1	13.711	-81.390	30	Uptake (nmol N l^{-1} h^{-1})	1.7(0.3)	0.1(0.1)	6.4(3.0)	7.1(3.1)	.05(0.0)
				Concentration (µM N)	2.5	0.2	0.3	1.4	0.01
				Turnover Time (days)	63	110	1.9	8.0	8.1
9	13.002	-82.198	2.5	Uptake (nmol N l^{-1} h^{-1})	3.5(4.3)	0.3(0.1)	5.8(2.4)	11(2.7)	0.2(0.0)
				Concentration (µM N)	1.1	0.1	0.1	0.6	0.01
				Turnover Time (days)	13	15	0.9	2.3	2.3
9	13.002	-82.198	30	Uptake (nmol N l^{-1} h^{-1})	2.5(3.3)	0.1(0.1)	7.8(0.8)	1.0(0.2)	0.2(0.2)
				Concentration (µM N)	1.0	0.1	0.1	BDL	0.01
				Turnover Time (days)	17	34	0.7	N/A	2.5

For Review Only

This article is protected by copyright. All rights reserved.

Table 2. N uptake rates in the oxygen deficient zone at station BB2 calculated using two methods- the Standard Uptake Calculation and the Time Series Calculation. The Standard Uptake Calculation is typically used to calculate uptake rates using a mixing model (Montoya et al. 1996; Mulholland et al. 2006; Mulholland and Lee 2009). For these, individual rates were calculated for each time point (A and B). Average deviations (n = 2 incubation bags) are shown in parentheses and p-values are the result of a two-tailed t-test where a bold value indicates a significant difference in uptake rate between time points A and B for $\alpha = 0.05$. The Time Series Calculation was used to calculate rates by fitting a linear regression to N taken up over time (Figure 11) as is standard for measurements of dissimilatory N processes such as anammox (Dalsgaard et al. 2003). Standard errors (n = 6 or 3[b]) are shown in parentheses, and p values shown in bold and italics indicate statistically significant linear uptake rates for $\alpha = 0.05$ and 0.1 criteria, respectively. Statistical parameters that could not be calculated due to low number of replicates are given as N/A.

		Standard Uptake Calculation					Time Series Calculation		
	Depth (m)	N Uptake (nmol N l^{-1} h^{-1})		Incubation Time (hours)		p	N Uptake (nmol N l^{-1} h^{-1})	R^2	p
		A	B	A	B				
OCN^-	95	0.07(0.03)	0.09(0.08)	8.6	36.3	0.78	0.08(0.04)	0.57	*0.076*
	230	0.14(0.02)	0.08(0.01)	25.9	47.9	0.11	0.08(0.03)	0.82	**0.010**
	400	0.29(0.16)	0.24(0.13)	10.5	28.8	0.77	0.23(0.03)	0.73	**0.024**
Urea	95	0.04(0.03)	0.18(0.07)	8.6	36.3	0.13	0.17(0.04)	0.86	**0.006**
	230	0.34(0.07)	0.24(0.03)	24.9	47.9	0.18	0.22(0.04)	0.92	**0.002**
	400	0.45(0.31)	0.35(0.08)	10.5	28.8	0.70	0.31(0.04)	0.86	**0.005**
NH_4^+	95	0.09(0.00)	0.16(0.01)	8.8	36.5	**0.01**	0.16(0.04)	0.98	**< 0.001**
	230 [a]	0.54[a]	0.36[a]	24.9	47.9	N/A	0.47(0.04)[b]	0.99	**< 0.001**
	400[a]	0.20[a]	0.58[a]	10.5	28.9	N/A	0.51(0.04)[b]	0.93	*0.072*

[a] There was only 1 incubation bag for this experiment.

Accepted Article For Review Only

This article is protected by copyright. All rights reserved.

Figure Legends

Figure 1. Station Map. Locations of all CTD casts (circles) and Stations 9, BB1, and BB2 (stars) overlain on satellite-derived sea surface temperature (averaged from July 2013; left panel). The longitudinal transect (Figs 2) and the transect parallel to the coastline (Figs 3) are shown in red and green boxes, respectively. Surface cyanate concentrations are shown in the right panel.

Figure 1 b/w for print edition. Station Map. Locations of all CTD casts (circles) and Stations 9, BB1, and BB2 (stars) overlain on satellite-derived sea surface temperature (averaged from July 2013; left panel). The longitudinal transect (Fig. 2) and the transect parallel to the coastline (Fig. 3) are indicated with the sold and dashed boxes, respectively. Surface cyanate concentrations are shown in the right panel.

Figure 2. Hydrographic parameters along a transect at 17 ^{o}S. Cyanate, ammonium, nitrite, nitrate, and chlorophyll *a* concentrations and potential density (sigma theta) are shown. Black dots and lines represent sampling locations and the colored contours represent interpolations of the given parameters between those data points. The 3 and 6 μM oxygen contours are shown (black contour lines), where 3 μM is approximately equal to the detection limit of the CTD oxygen sensor and delineates the extent of the oxygen deficient zone. The left side (0 km) represents the northernmost station and the right side (1500 km) represents the southernmost station. See Figure 1 for station locations.

Figure 2 b/w for print edition. Hydrographic parameters along a transect at 17 ^{o}S. Cyanate, ammonium, nitrite, nitrate, and chlorophyll *a* concentrations and potential density (sigma theta) are shown. Black dots and lines represent sampling locations and the grey shading and white contours represent interpolations of the given parameters between those data points. The white contour lines are only shown for the upper 150 m. The 3 and 6 μM oxygen contours are shown (black contour lines), where 3 μM is approximately equal to the detection limit of the CTD oxygen sensor and delineates the extent of the oxygen deficient zone. The left side (0 km) represents the northernmost station and the right side (1500 km) represents the southernmost station. See Figure 1 for station locations.

Figure 3. Hydrographic parameters along a transect parallel to the coastline. Cyanate, ammonium, nitrite, nitrate, and chlorophyll *a* concentrations and potential density (sigma theta) are shown. Black dots and lines represent sampling locations and the colored contours represent interpolations of the given parameters between those data points. The 3 and 6 μM oxygen contours are shown (black contour lines), where 3 μM is approximately equal to the detection limit of the CTD oxygen sensor and delineates the extent of the oxygen deficient zone. The left side (0 km) represents the northernmost station and the right side (1500 km) represents the southernmost station. See Figure 1 for station locations.

Accepted Article

This article is protected by copyright. All rights reserved.

Figure 3 b/w for print edition. Hydrographic parameters along a transect parallel to the coastline. Cyanate, ammonium, nitrite, nitrate, and chlorophyll *a* concentrations and potential density (sigma theta) are shown. Black dots and lines represent sampling locations and the grey shading and white contour lines represent interpolations of the given parameters between those data points. The white contour lines are only shown for the upper 100 m. The 3 and 6 µM oxygen contours are shown (black contour lines), where 3 µM is approximately equal to the detection limit of the CTD oxygen sensor and delineates the extent of the oxygen deficient zone. The left side (0 km) represents the northernmost station and the right side (1500 km) represents the southernmost station. See Figure 1 for station locations.

Figure 4. Vertical distributions and uptake rates for station BB1. A) Chlorophyll *a* (Chl *a*, mg m^{-3}) is shown in grey and oxygen concentrations (umol kg^{-1}) are shown in black. B) Nitrate (NO_3^-) and nitrite (NO_2^-) concentrations (µM) are shown with a dotted line and solid line, respectively, and uptake rates of NO_3^- and NO_2^- are shown with closed and open circles, respectively. In panels C-E concentrations (nM) of cyanate (OCN^-), urea, and ammonium (NH_4^+) are depicted by the solid lines, and uptake rates of OCN^-, urea, and NH_4^+ (nmol N l^{-1} h^{-1}) are depicted with closed circles. Concentrations and uptake rates below the detection limit were plotted as equal to the detection limit (0.6 nM for OCN^-, 80 nM for urea, 50 nM for NH_4^+, and 70 nM for NO_2^- and NO_3^-). Error bars are ± 1 standard deviation for OCN^- concentrations (n=3) and ± 1 average deviation for uptake rates (n=2).

Figure 5. Vertical distributions, uptake rates, and anammox rates for station BB2. A) Chlorophyll *a* fluorescence (Chl *a*, mg m^{-3}) is shown in grey and oxygen (µmol kg^{-1}) is shown in black. B) Nitrate (NO_3^- µM) is shown with a dotted line and nitrite (NO_2^-, µM) is shown with a solid line. In panels C-E concentration (nM) is depicted by the solid line (samples collected every 4 m), uptake rate from the first time point (nmol l^{-1} h^{-1}) is depicted with closed circles connected by dashed lines, and rate of $^{15}N_2$ production from cyanate (OCN^-), urea, and ammonium (NH_4^+, nmol l^{-1} h^{-1}) is depicted by open circles. Concentrations and uptake rates below the detection limit were plotted as equal to the detection limit (0.6 nM for OCN^-, 80 nM for urea, and 10 nM for NH_4^+). Error bars are ± 1 standard deviation (concentration, $^{15}N_2$ production, n=3) and ± 1 average deviation (uptake, n=2). $^{15}N_2$ production rates and NO_3^-, NO_2^-, and oxygen profiles are reproduced from Babbin et al (2017).

Figure 6. N uptake at two offshore stations. Total N uptake is the sum of ammonium (NH_4^+, white), nitrate (NO_3^-, black), nitrite (NO_2^-, hatched), urea-N (grey), and cyanate (OCN^-, black and white checked) uptake. See Table 1 for uptake rates including error.

Figure 7. Cyanate uptake kinetics. Cyanate uptake at station BB1 in surface water (closed circles, R^2 = 0.9981) and at water collected from the chlorophyll *a* maximum (30 m; chl a max) (open circles, R^2 = 0.9928), and at station BB2 in surface water (diamonds, R^2 = 0.9995). Error bars are ± 1 standard deviation (n = 2). Where error bars are not visible they are smaller than the symbol.

Accepted Article

This article is protected by copyright. All rights reserved.

Figure 8. Diurnal cyanate uptake at station BB2. Samples were collected from the ship's seawater flow-through system on July 18 and 19, 2013 to measure cyanate uptake. N uptake rates are reported in nmol N l^{-1} h^{-1} (closed circles) and nmol N μg (Chl *a*)$^{-1}$ h^{-1} (open circles), and C uptake rates are reported in nmol C l^{-1} h^{-1} (closed diamonds) and nmol C μg (Chl *a*)$^{-1}$ h^{-1} (open diamonds). Times are local with shading indicating nighttime. Error bars are ± 1 average deviation (*n*=2) and time is the mean of the incubation length for ~ 2 hour incubations. Carbon uptake rates that were BDL are reported as equal to the average detection limit (0.02 nmol C l^{-1} h^{-1}).

Figure 9. Uptake of cyanate (OCN^-, A), urea (B) and ammonium (NH_4^+, C) N in the oxygen deficient zone at the first anoxic depth (95 m), at the secondary nitrite maximum (230 m), and just above the base of the ODZ (400 m). All incubations were performed at station BB2 in gas tight bags which were sampled at two time points. Replicate bags are represented by grey diamonds and black circles, and the uptake rate was calculated as the slope of the line of the average of all replicates (solid line). Statistical parameters and uptake rates are shown in Table 2.

Accepted Article

This article is protected by copyright. All rights reserved.

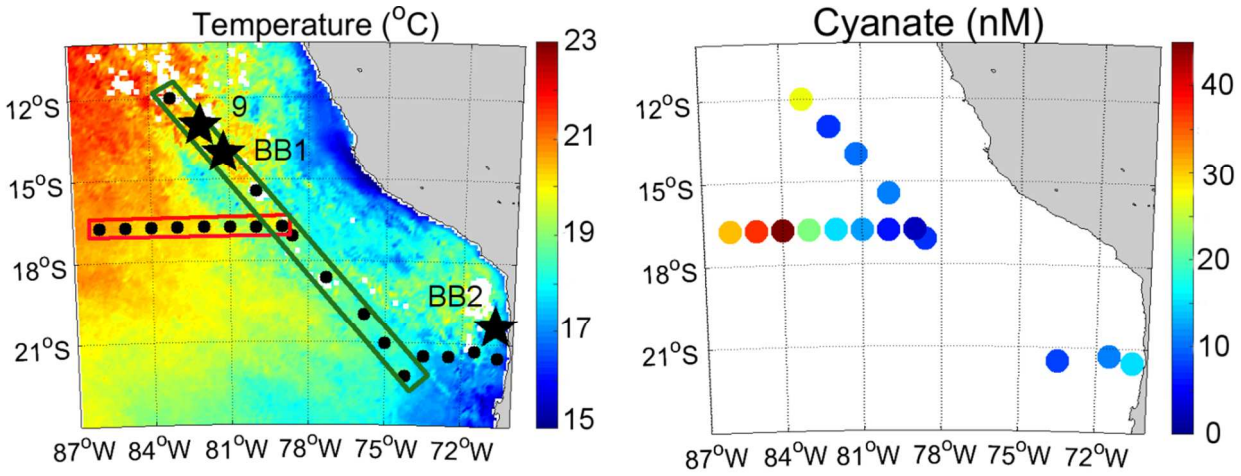

Accepted Ar

This article is protected by copyright. All rights reserved.

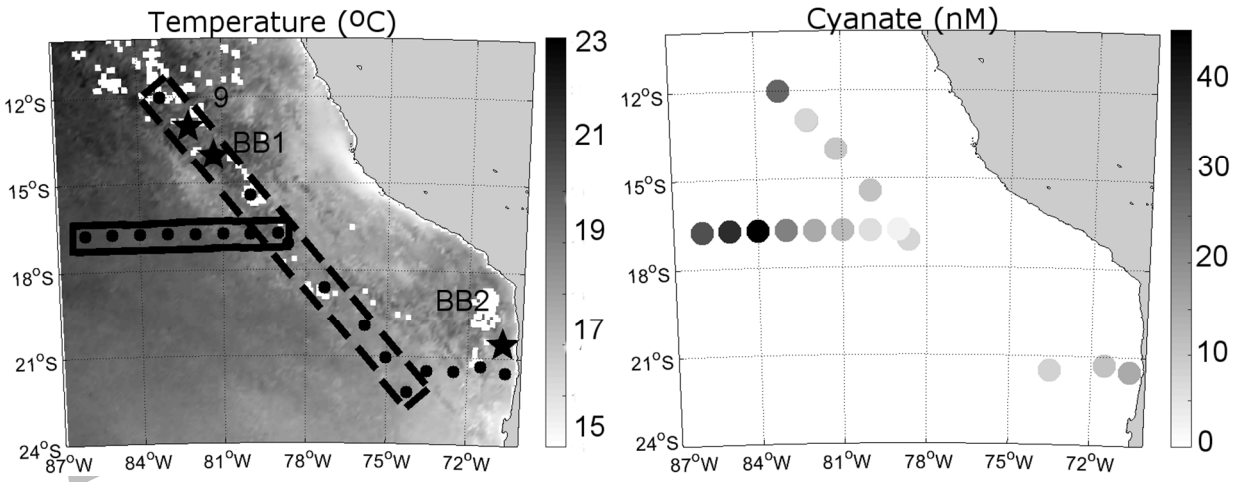

Accepted Ar

This article is protected by copyright. All rights reserved.

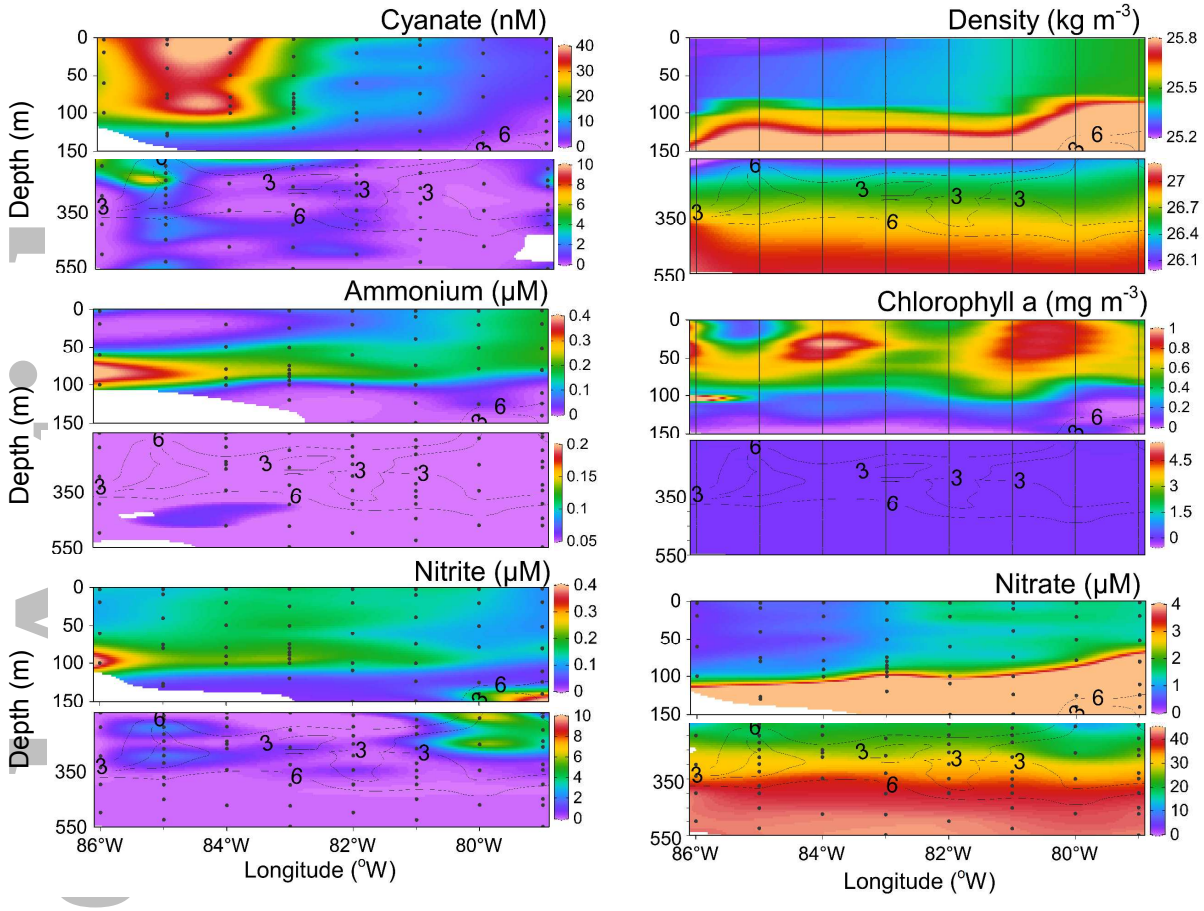

Accepted

This article is protected by copyright. All rights reserved.

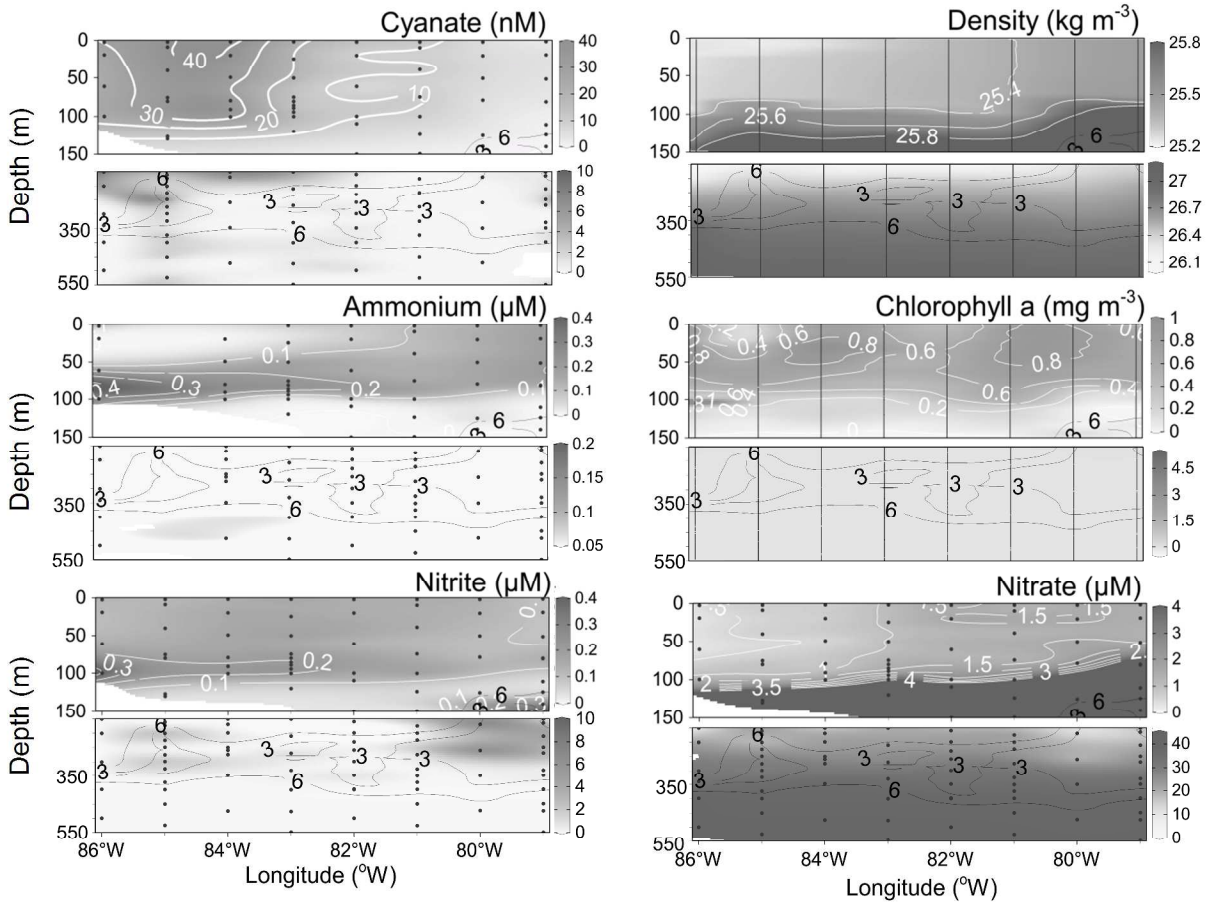

This article is protected by copyright. All rights reserved.

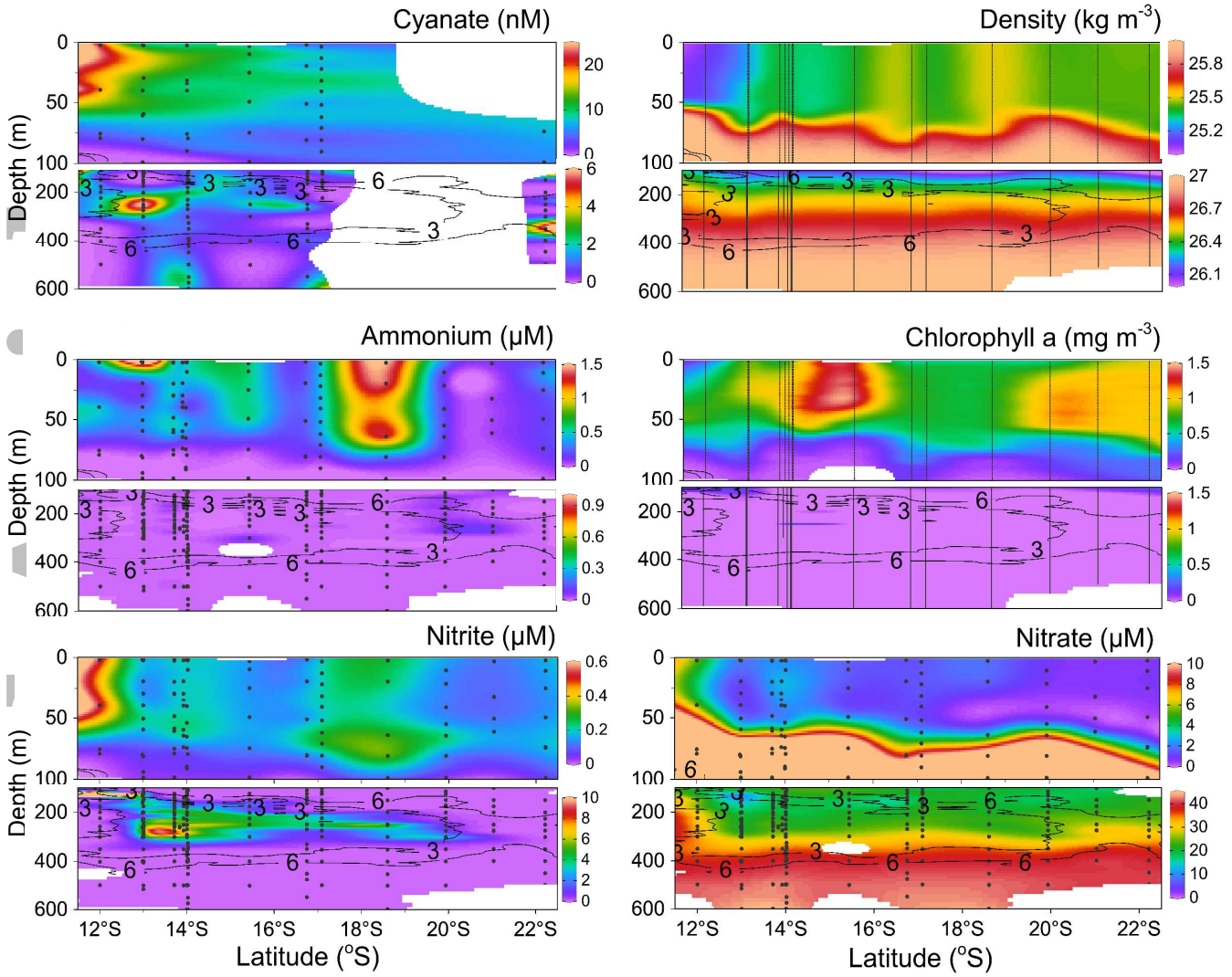

Accepted

This article is protected by copyright. All rights reserved.

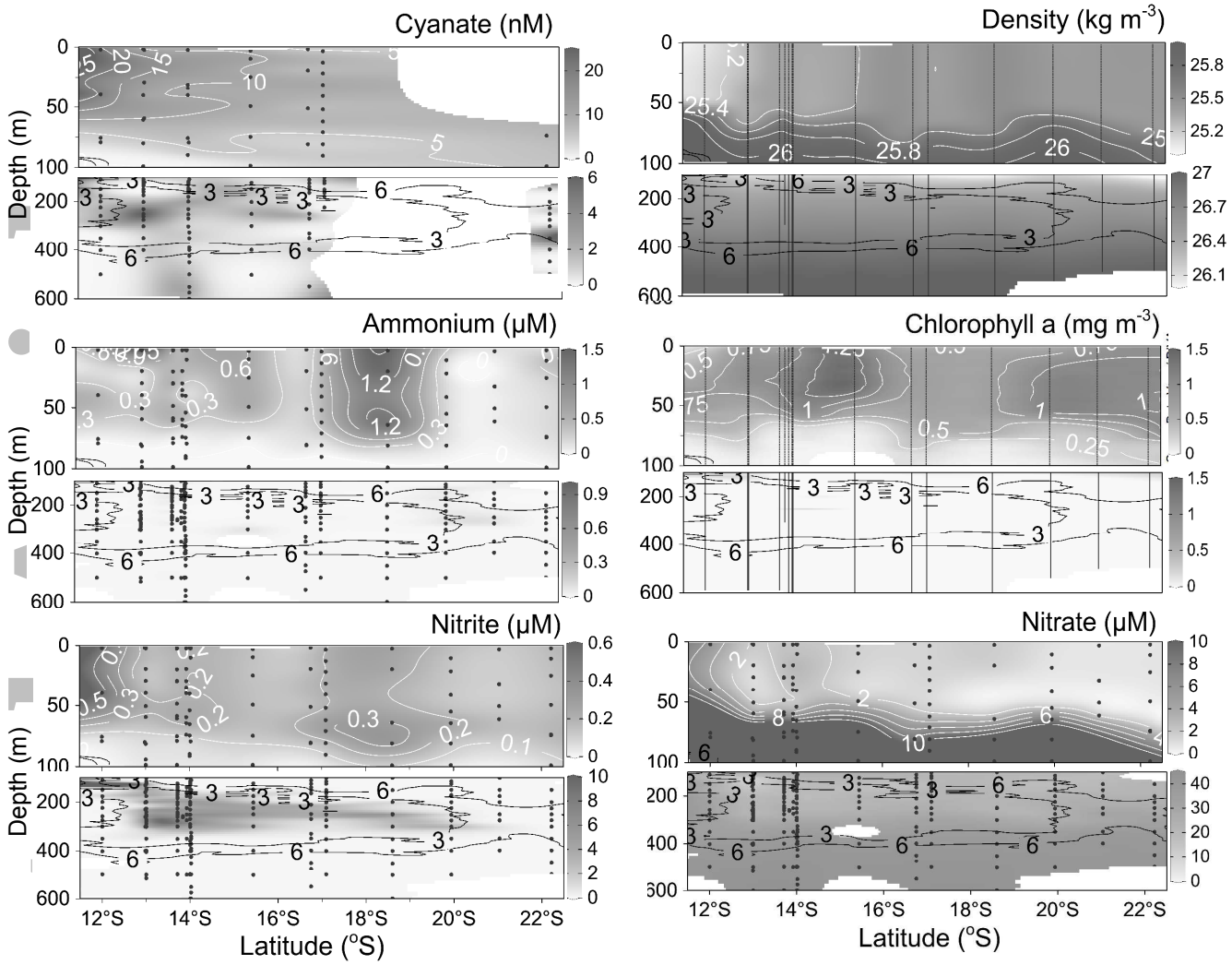

Accepted

This article is protected by copyright. All rights reserved.

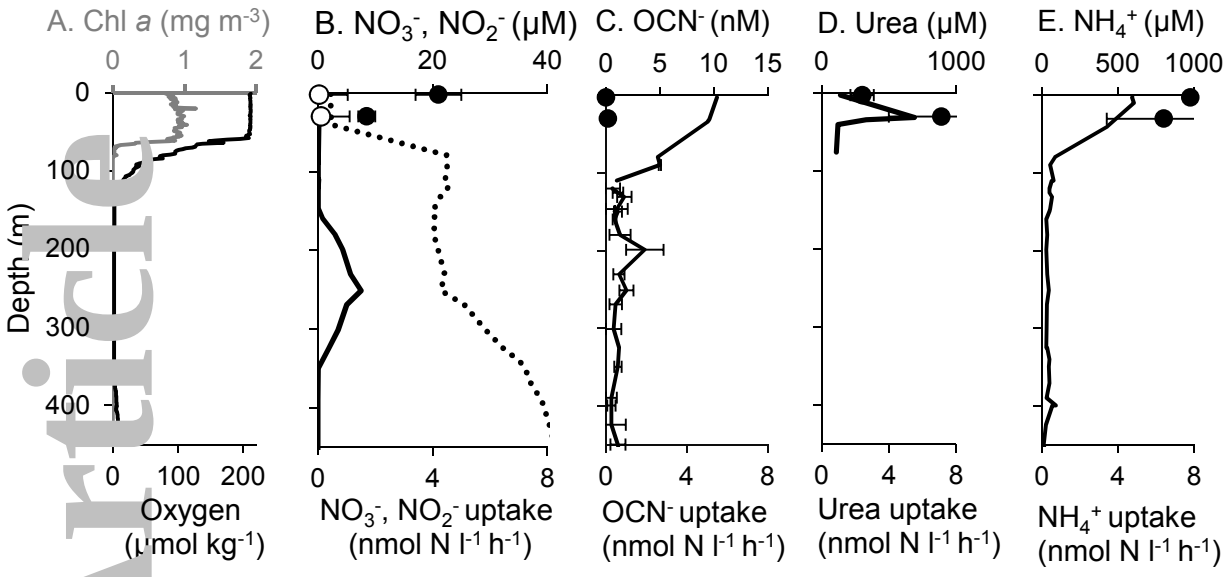

Accepted Article

This article is protected by copyright. All rights reserved.

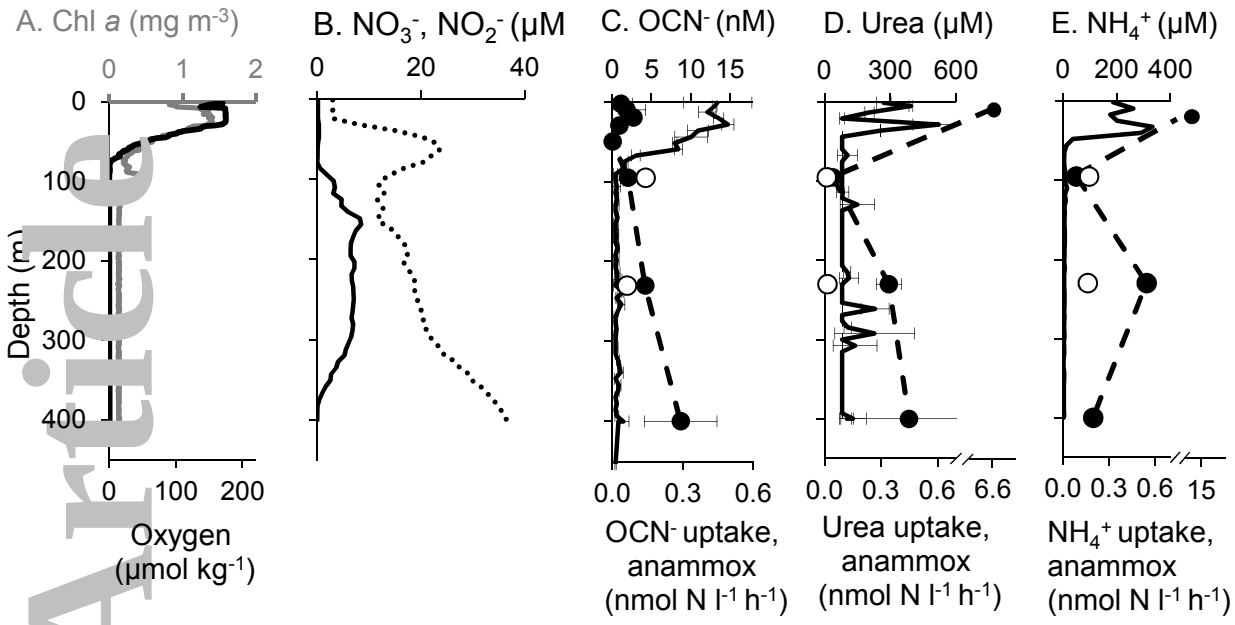

Accepted Article

This article is protected by copyright. All rights reserved.

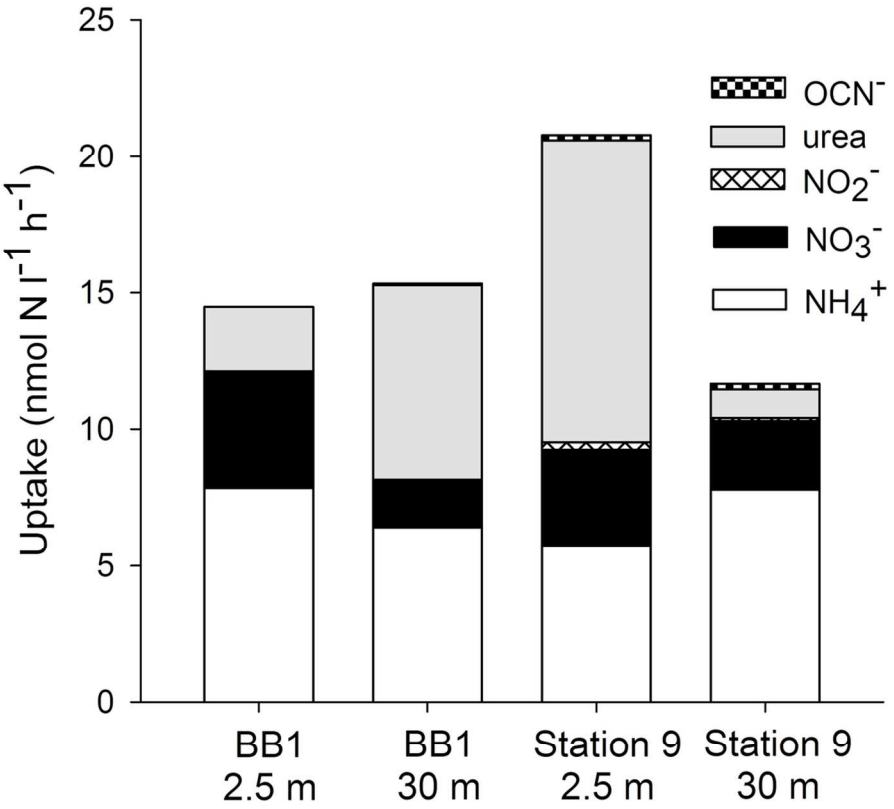

Figure 6. N uptake at two offshore stations. Total N uptake is the sum of ammonium (NH4+, white), nitrate (NO3-, black), nitrite (NO2-, hatched), urea-N (grey), and cyanate (OCN-, black and white checked) uptake. See Table 1 for uptake rates including error.

114x101mm (300 x 300 DPI)

Acc

This article is protected by copyright. All rights reserved.

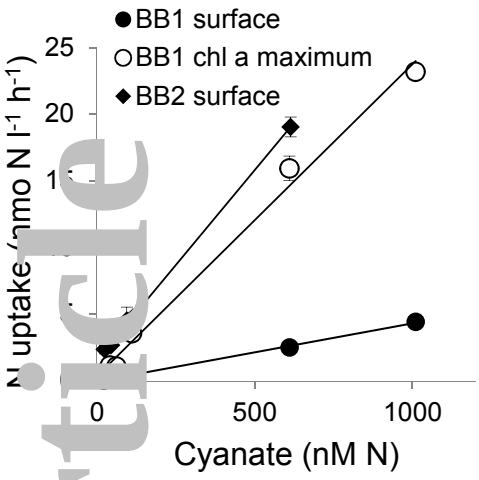

Accepted Article

This article is protected by copyright. All rights reserved.

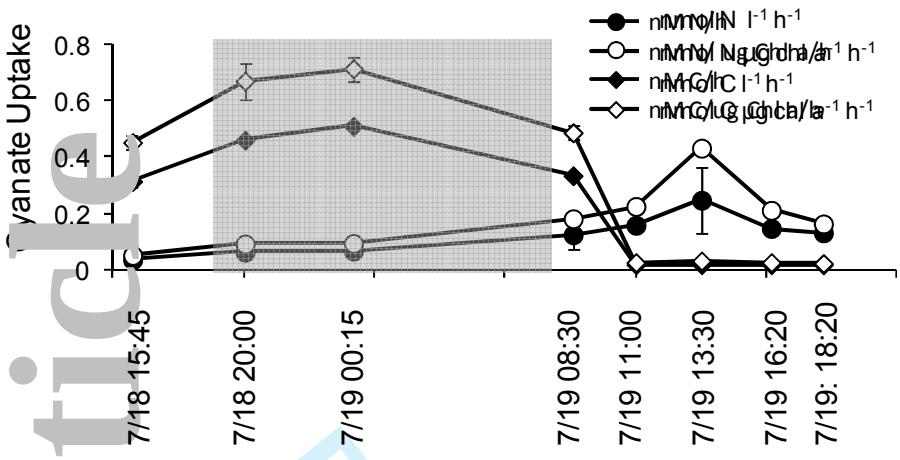

Accepted Article
For Review Only

This article is protected by copyright. All rights reserved.

A. OCN^-

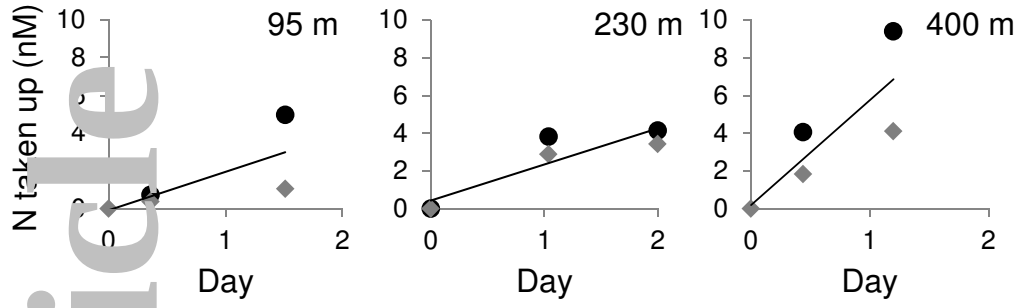

B. Urea

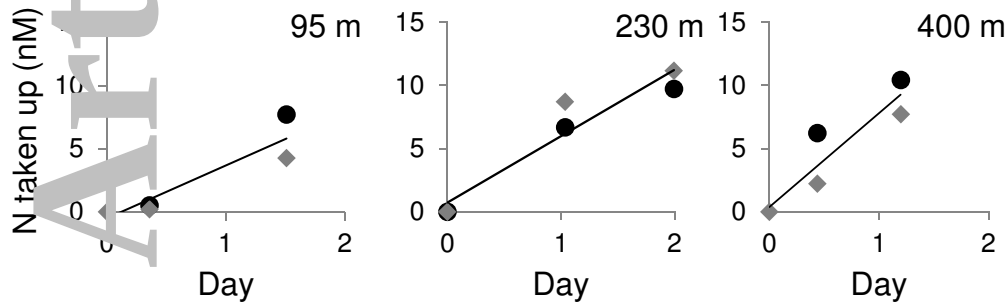

C. NH_4^+

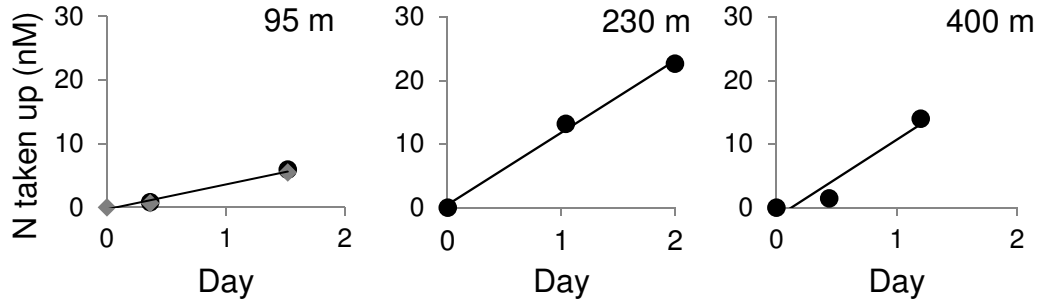

Accepted Article

This article is protected by copyright. All rights reserved.